Contrib Mineral Petrol (2001) 140: 734–753
DOI 10.1007/s004100000221

F. V. Kaminsky · O. D. Zakharchenko · R. Davies
W. L. Griffin · G. K. Khachatryan-Blinova
A. A. Shiryaev

Superdeep diamonds from the Juina area, Mato Grosso State, Brazil

Received: 29 May 2000 / Accepted: 30 October 2000 / Published online: 9 February 2001

Abstract Alluvial diamonds from the Juina area in Mato Grosso, Brazil, have been characterized in terms of their morphology, syngenetic mineral inclusions, carbon isotopes and nitrogen contents. Morphologically, they are similar to other Brazilian diamonds, showing a strong predominance of rounded dodecahedral crystals. However, other characteristics of the Juina diamonds make them unique. The inclusion parageneses of Juina diamonds are dominated by ultra-high-pressure (''superdeep'') phases that differ both from ''traditional'' syngenetic minerals associated with diamonds and, in detail, from most other superdeep assemblages. Ferropericlase is the dominant inclusion in the Juina diamonds. It coexists with ilmenite, Cr-Ti spinel, a phase with the major-element composition of olivine, and SiO_2. CaSi-perovskite inclusions coexist with titanite (sphene), ''olivine'' and native Ni. MgSi-perovskite coexists with TAPP (tetragonal almandine-pyrope phase). Majoritic garnet occurs in one diamond, associated with CaTi-perovskite, Mn-ilmenite and an unidentified Si-Mg phase. Neither Cr-pyrope nor Mg-chromite was found as inclusions. The spinel inclusions are low in Cr and Mg, and high in Ti ($Cr_2O_3 < 36.5$ wt%, and $TiO_2 > 10$ wt%). Most ilmenite inclusions have low MgO contents, and some have very high (up to 11.5 wt%) MnO contents. The rare ''olivine'' inclusions coexisting with ferropericlase have low Mg# (87–89), and higher Ca, Cr and Zn contents than typical diamond-inclusion olivines. They are interpreted as inverted from spinel-structured $(Mg, Fe)_2Si_2O_4$. This suite of inclusions is consistent with derivation of most of the diamonds from depths near 670 km, and adds ilmenite and relatively low-Cr, high-Ti spinel to the known phases of the superdeep paragenesis. Diamonds from the Juina area are characterized by a narrow range of carbon isotopic composition ($\delta^{13}C = -7.8$ to $-2.5‰$), except for the one majorite-bearing diamond ($\delta^{13}C = -11.4‰$). There are high proportions of nitrogen-free and low-nitrogen diamonds, and the aggregated B center is predominant in nitrogen-containing diamonds. These observations have practical consequences for diamond exploration: Low-Mg olivine, low-Mg and high-Mn ilmenite, and low-Cr spinel should be included in the list of diamond indicator minerals, and the role of high-Cr, low-Ti spinel as the only spinel associated with diamond, and hence as a criterion of diamond grade in kimberlites, should be reconsidered.

F. V. Kaminsky (✉)
1KM Diamond Exploration, 815 Evelyn Drive,
West Vancouver V7 T 1J1, B.C., Canada
E-mail: felixvkaminsky@cs.com

O. D. Zakharchenko · G. K. Khachatryan-Blinova
Institute of Diamonds Ltd., Ste. 155–5/10 Litovskii Blvd.,
Moscow 117593, Russia

F. V. Kaminsky · R. Davies · W. L. Griffin
GEMOC Key Centre, Department of Earth and Planetary
Sciences, Macquarie University, Sydney 2109, Australia

W. L. Griffin
CSIRO Exploration and Mining, P.O. Box 128,
North Ryde, NSW 1609, Australia

A. A. Shiryaev
Vernadsky Institute of Geochemistry and Analytical Chemistry,
Kosygin St. 19, Moscow 117975, Russia

Editorial responsibility: W. Schreyer

Introduction

The Juina area is a major diamond mining area in Brazil (Fig. 1). In the late 1980s–early 1990s, as many as 50,000 artisanal miners (garimpeiros) worked this area, producing up to 5–6 million carats of diamonds each year according to local sources of information. Many of the diamonds recovered during this period were larger than 100–200 carats, with the largest reported stone weighing up to 480 ct (Gaspar et al. 1998). There are at least 26 kimberlite pipes in the area. Some of them are subeconomic with up to 0.5 ct t^{-1} diamond grade. However, all diamond production has been from recent alluvial and colluvial deposits.

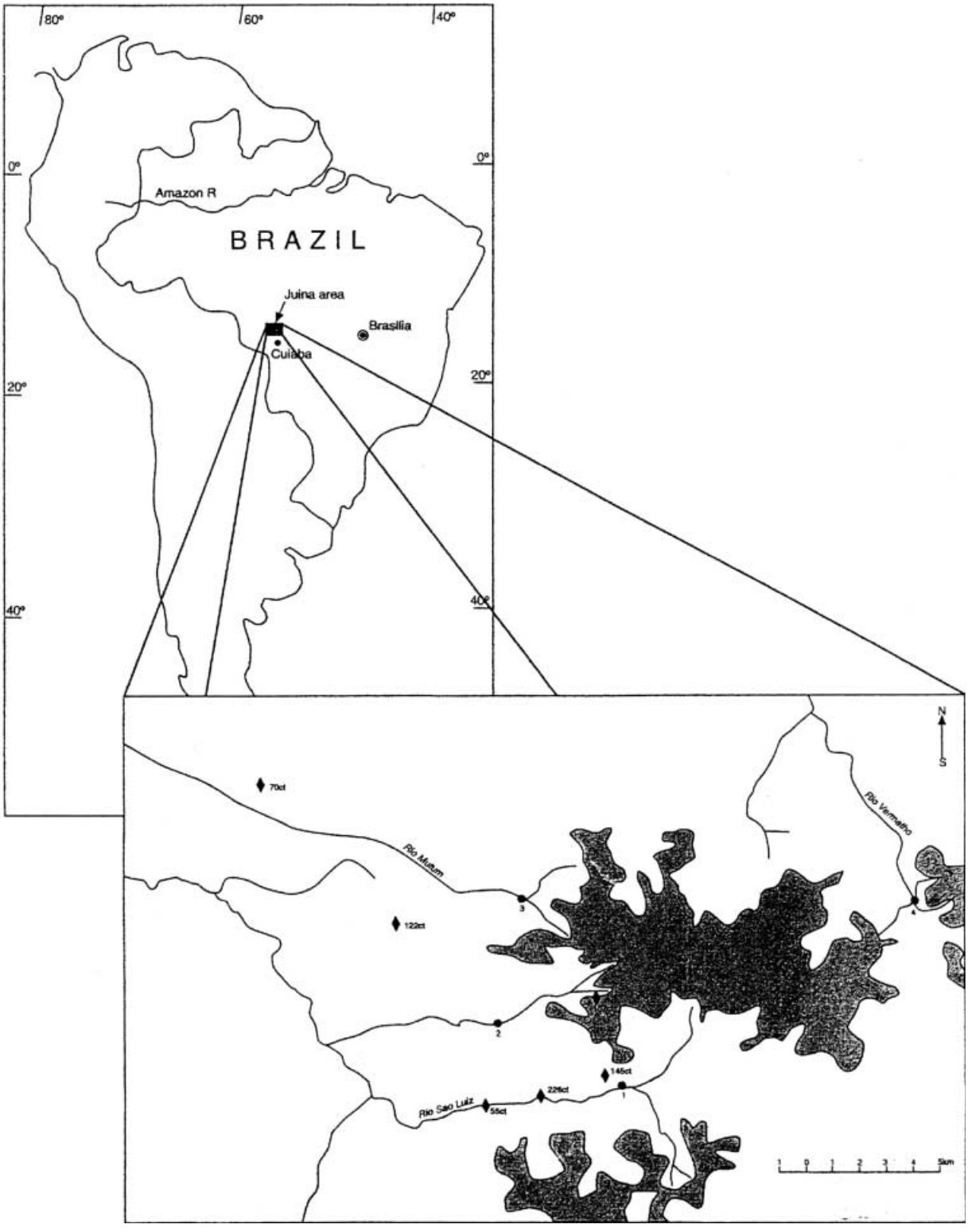

Fig. 1 Location and sketch map of the Juina area. *Black circles* Diamond sample sites; *black diamonds* finds of large diamonds (in carats); *shaded area* Cretaceous-Tertiary ''Chapada'' deposits

Diamonds from this area have attracted considerable attention because several studies by J.W. Harris, B. Harte and coworkers (summarized by Harte et al. 1999) have documented the presence, in diamonds from the Sao Luiz drainage, of a mineral inclusion paragenesis that suggests derivation from the lower mantle at depths of at least 660 km.

We have studied a set of 475 diamonds, from 0.01–5.3 ct in weight, from several drainages within the Juina area (Fig. 1). These include the Rio Sao Luiz [sample

area ''1''; this probably includes the source of the Sao Luiz diamonds studied by Harte et al. (1999)], the Rio Mutum (sample area ''3''), the Rio Vermelho (sample area ''4''), and Corrigo Chicora (sample area ''5''). The sample numbers used in the text below and in the tables give the area number (the first part) and the stone number (the second part).

Morphologically, diamonds from the Juina area are similar to other Brazilian diamonds, showing a strong predominance of rounded dodecahedral crystals. However, other characteristics of the Juina diamonds, such as their mineral inclusions, their carbon isotopic composition and their uniformly low nitrogen contents, combine to make them unique with respect to other diamond populations.

The data presented here expand the range of mineral associations in diamonds from the transition zone and lower mantle, which can be recognized as a ''superdeep'' parageneses, distinct from the more common peridotitic and eclogitic parageneses found in diamonds from the subcontinental lithosphere. They further define the carbon-isotope and nitrogen impurity characteristics of diamonds from the transition zone and lower mantle.

Analytical methods

Major-element data on mineral inclusions have been obtained using two instruments, and the source of each analysis is marked in the data tables. Analyses produced at the Department of Earth and Planetary Sciences, Macquarie University, were done on a CAMEBAX SX50 electron microprobe using a range of natural and synthetic mineral standards. Similar data from this microprobe have been independently verified by cross analysis in Australia (CSIRO) and Norway (Mineralogical-Geological Museum). Other analyses were carried out by the Institute of Diamonds using a CAMEBAX instrument in a commercial laboratory.

The trace-element analyses used in this report have been obtained with a laser-ablation ICPMS microprobe (LAM-ICPMS) at the Department of Earth and Planetary Sciences, Macquarie University. The LAM analyses were carried out using methods described in detail by Norman et al. (1996, 1998). The instrument uses an Nd-YAG infrared laser, frequency-quadrupled to produce a beam of UV (266-nm) light which is focused through a petrographic microscope onto a polished grain or thin section in the sample cell. The gas flowing through the cell carries the ablated sample to a Hewlett-Packard 4500 ICPMS. The external standard for the analyses reported here was the NIST 612 glass. Ca was used as the internal standard for garnet analyses, and Mg or Al for the other phases. Typical ablation pits were 40 μm in diameter and up to 50 μm deep. Detection limits for most elements are from 1 ppm to 10 ppb, and precision at these levels is typically better than 10% (Norman et al. 1996, 1998).

Most carbon-isotope analyses were carried out at the Vernadsky Institute, Moscow, using standard techniques (Galimov 1985). Samples were converted to CO_2 by oxygen released from CuO at a temperature of 800° C in a vacuum system. The CO_2 was analyzed using a MAT230 mass spectrometer with a typical precision of 0.1‰. Isotopic composition is given in delta notation (parts per thousand) as the deviation from the PDB standard. Several supplementary analyses were carried out at the Division of Petroleum Resources, CSIRO (North Ryde), using methods described previously by Davies et al. (1999).

Infrared (IR) spectra were obtained at the Institute of Diamonds in Moscow, using a Specord M-80 spectrometer (Karl Zeiss, Jena) with a beam condenser. Spectral resolution was 6–10 cm^{-1}. Concentrations of A and B nitrogen centers were calculated according to the IR absorption coefficients specified by Boyd et al. (1994, 1995).

No crystal-structure determinations by X-ray diffraction have been carried out on the mineral inclusions reported here. The mineral identifications therefore are based solely on chemical analysis, optical data and mineral associations.

Diamond morphology and coloration

Morphologically, the Juina diamonds are very homogeneous. Dodecahedroids are most common (55–70% of the diamonds in the sample), and diamonds of irregular shape account for approximately one third of the total sample. Minor morphological types include octahedra (about 5%) and diamonds with combinations of forms (4–7.5%). Dodecahedroids are complexly distorted. A distinctive feature of dodecahedroid diamonds from the Juina area is that their surfaces show only shagreen microrelief. This is in contrast to the wide variety of surface features generally present on diamonds from other regions, including placer deposits in Minas Gerais. The crystals are commonly smoky brown (from pale, almost colorless, to dark brown) and semitransparent with a silky luster. They show abundant plastic deformation bands and etch channels.

Mineral inclusions in diamonds

Examination of the syngenetic mineral inclusions in the Juina diamonds reveals that they are dominated by phases of the superdeep paragenesis, in contrast to most other diamond suites worldwide. Fourteen different phases, identified by their chemical composition and optical properties, were found as inclusions in the Juina-area diamonds: ferropericlase (fPer), MgSi-perovskite (MgSiPvk), CaSi-perovskite (CaSiPvk), CaTi-perovskite (CaTiPvk), sphene ($CaTiSiO_5$), TAPP, SiO_2, low-Mg ilmenite, picroilmenite, low-Cr, high-Ti spinel, majoritic garnet, native Ni, unidentified Si-Mg phase, and a phase with the major-element composition of olivine. Minor-element data and mineral association (see below) indicate that this phase cannot originally have been olivine. In the absence of XRD data, it is possible that the ''MgSiPvk'', ''CaTiPvk'' and ''CaTiPvk'' inclusions, after retrograde phase transformations, no longer have the perovskite structure, as suggested by Joswig et al. (1999).

Ferropericlase coexists in single diamonds with ilmenite, spinel, ''olivine'' and SiO_2. CaSiPvk coexists with sphene, and MgSiPvk coexists with TAPP. Majoritic garnet coexists with CaTiPvk and Mn-ilmenite. Neither chromite nor Cr-pyrope garnet was found as inclusions. A total of 68 mineral inclusions were extracted by cracking from 48 Juina diamonds and analyzed (Table 1).

Table 1 Mineral inclusions in the Juina diamonds

Mineral inclusions and associations	Number of diamonds (sample no.)
Monomineral inclusions	
Fe-periclase	20 (incl. three grains in no. 3–15, and two grains in no. 5–103)
Ilmenite	8
Picroilmenite	3
Spinel	3
CaSi-perovskite	1
"Olivine"	1
SiO_2	2
Associations	
Fe-periclase + ilmenite	2 (no. 1–4, and 1–7)
Fe-periclase + spinel	1 (no. 5–17 with two spinel grains)
Fe-periclase + "olivine"	1 (no. 5–5)
Fe-periclase + SiO_2	1 (no. 5–102 – touching)
CaSi-perovskite + Ni	1 (no. 5–104 with three CaSi-perovskite grains)
CaSi-perovskite + "olivine"	1 (no. 4–101)
CaSi-perovskite + "titanite"	1 (no. 5–101 – touching)
MgSi-perovskite + TAPP	1 (no. 4–104 – touching)
Majorite + ilmenite + CaTi-perovskite + Si-Mg phase	1 (no. 5–108 with three majorite grains)
Total: 14 minerals	48 diamonds with 68 mineral inclusions

Ferropericlase

Ferropericlase (fPer) is the most abundant inclusion phase in the diamonds studied. Twenty-eight ferropericlase inclusions were extracted from 25 diamonds. They have equidimensional to flattened, sometimes irregular shapes, and range in size from 0.05 to 0.45×0.30 mm. The chemical compositions of ferropericlase inclusions from the Juina area range in mg [= Mg/(Mg + Fe)] from 0.491–0.826 (corresponding to a variation in FeO from 62.42–26.39%; Table 2, Fig. 2). This is within the wider range (mg = 0.38–0.85) reported for 24 ferropericlases from Sao Luiz (Harte et al. 1999). Three ferropericlase grains from a single diamond (no. 3–15) show a significant range in mg from 0.609–0.746. Harte et al. (1999) report a range of 0.634–0.819 for two ferropericlase inclusions in a single diamond from Sao Luiz. This shows that disequilibrium among inclusions in single diamonds is common not only in the upper mantle, but in the lower mantle as well.

The ferropericlases have almost stoichiometric (Mg, Fe)O composition, with some interesting features in minor-element contents (Table 2). As a rule, the most iron-rich ferropericlases have higher MnO contents which reach 0.85 wt%. A maximum of 0.8% MnO has been reported in the Sao Luiz ferropericlases by Harte et al. (1999). TiO_2 contents are 0–0.07 wt% in most cases. In grain no. 1–4, ferropericlase associated with ilmenite contains 0.24% TiO_2, the highest value yet reported. The highest Cr_2O_3 content is 2.26 wt% (no. 5–5), similar to the 2.56% Cr_2O_3 reported by Harte et al. (1999). Na_2O contents reach 1.35 wt% (sample no. 5–21), similar to the 1.25% found by Harte et al. (1999). The Ni content of ferropericlase is positively correlated with MgO content, and NiO contents up to 1.37% are found in the ferropericlases with $mg > 0.7$. Most non-Brazilian fPer inclusions have Ni contents at the upper end of the range found in the Juina fPer inclusions (Fig. 2).

The trace-element analyses show that the fPer has low average contents of the REE and other LILE (large ion lithophile elements), but near-chondritic abundances of several transition elements (Sc, V, Cr, Mn, Co) and elevated abundances of some HFSE (high field strength elements; Ti, Zr, Nb, Ta), as well as U and Th (Table 2, Fig. 3). Mn and Cr contents are negatively correlated with Mg#, whereas Na shows a weak positive correlation with Mg#. Li abundances are high (5–10x chondrites). The abundances of the LILE and HFSE are highly variable, with some analyses showing high levels, and others very low levels.

Ilmenite

Ilmenite inclusions are 0.05 to 0.40×0.30 mm in size. The 14 ilmenite grains analyzed can be subdivided into low-Mg ilmenite and picroilmenite (Table 2). Low-Mg ilmenites, with MgO contents less than 0.82 wt%, are the predominant type in the Juina diamonds (11 of the 14 ilmenites analyzed). Low-Mg ilmenite inclusions were reported by Meyer and Svisero (1980) in Brazilian diamonds which were probably from the Juina area. Low-Mg and high-Mn ilmenite inclusions have also been found in a few Venezuelan diamonds (Kaminsky et al. 1997; Sobolev et al. 1998). One of the Mn-rich ilmenites (no. 1–7) from the Juina area occurs in the same diamond as a ferropericlase inclusion; another (no. 5–108) occurs together with three grains of majoritic garnet and a CaTi-perovskite. Four of the 11 low-Mg ilmenites from the Juina diamonds (nos. 1–7, 1–8, 1–32, and 5–108) have very high MnO contents (2–11 wt%). Several of the high-Mn ilmenites are heterogeneous. In a large inclusion from diamond no. 1–7, MnO ranges from 4.8–11.5%, and Mn is irregularly distributed within the grain. This pattern may suggest unmixing of the grain

Table 2 Oxide mineral composition for Juina diamond inclusions (for the native Ni inclusion all figures are element contents). *MU* Analyzed at Macquarie University; *ID* analyzed in the Institute of Diamonds; *n.a.* not analyzed

Mineral	fPer	fPer	fPer	fPer	fPer	fPer	fPer	fPer	fPer	fPer	fPer	fPer	fPer	fPer	fPer	fPer	fPer	fPer	fPer	fPer	fPer	fPer	fPer
Sample no.	1–4	1–7	1–31	1–33	1–36	1–38	3–1	3–2	3–3	3–4	3–5	3–6	3–10	3–15a	3–15b	3–15c	3–16	3–101	4–18	4–33	5–5	5–7	5–17	5–21
Association	Ilm	Ilm																			"Olivine"		Spinel	
Analyzed	MU	ID	MU	MU	MU	MU	MU	MU	MU	ID	ID	MU	MU	MU	MU	MU	MU	MU	MU	MU	MU	MU	ID	MU
No. of anal.	3	3	3	3	2	3	3	1	1	3	3	3	3	3	1	3	3	3	3	3	1	3	3	3
Wt%																								
SiO_2	0.15		0.01	0.02	0.01	0.01	0.00	0.05	0.00			0.01	0.02	0.01	0.00	0.02	0.01	0.01	0.02	0.03	0.01	0.05		0.01
TiO_2	0.24	<0.03	<0.03	<0.03	0.02	<0.03	0.03	<0.03	0.05	<0.03		<0.03	<0.03	<0.03	<0.03	<0.03	<0.03	<0.03	<0.03	0.05	<0.03	0.07		<0.03
Al_2O_3	0.29	0.51	0.08	0.07	0.03	0.06	0.07	0.08	0.08	0.10	0.08	0.10	0.09	0.07	0.05	0.07	0.05	0.05	0.08	0.11	0.25	0.23	0.13	0.17
Cr_2O_3	0.78	0.95	0.11	0.51	1.75	0.58	0.69	0.70	0.85	0.68	0.71	0.63	0.72	0.68	0.37	0.16	0.17	0.52	0.70	0.29	2.26	1.70	0.72	1.16
FeO_{tot}	46.76	35.56	58.23	26.39	62.42	38.39	52.18	41.81	52.40	50.44	48.75	28.82	51.67	51.49	36.88	41.70	41.34	45.46	52.39	35.19	34.96	41.60	50.38	51.91
NiO	1.03		0.40	1.17	0.02	1.19	0.89	0.79	0.60			1.33	0.87	0.83	1.11	0.98	0.98	0.87	0.80	1.37	0.71	1.34		0.44
MnO	0.26	0.27	0.34	0.25	0.69	0.41	0.43	0.39	0.47	0.49	0.40	0.35	0.40	0.39	0.32	0.24	0.19	0.40	0.42	0.25	0.50	0.58	0.46	0.51
MgO	49.78	62.85	39.66	70.37	33.80	58.26	44.56	56.98	44.50	48.66	50.25	66.66	45.07	44.98	60.63	56.80	56.45	52.64	44.74	62.27	59.08	53.45	48.13	44.03
CaO	<0.03		<0.03	<0.03	<0.03	<0.03	<0.03	<0.03	<0.03			<0.03	<0.03	<0.03	<0.03	<0.03	<0.03	<0.03	<0.03	<0.03	<0.03	<0.03		<0.03
Na_2O	<0.04		<0.04	0.04	0.39	0.58	0.90	0.37	0.39			0.20	0.84	0.87	0.08	0.04	<0.04	0.47	0.83	0.13	1.14	0.54		1.35
K_2O	<0.04		<0.04	<0.04	<0.04	<0.04	<0.04	<0.04	<0.04			<0.04	<0.04	<0.04	<0.04	<0.04	<0.04	<0.04	<0.04	<0.04	<0.04	<0.04		
Total	99.27	100.14	98.83	98.83	99.13	99.49	99.75	101.16	99.34	100.37	100.19	98.10	99.68	99.31	99.44	100.00	99.19	100.42	99.99	99.69	98.91	99.57	99.82	99.57
mg	0.655	0.759	0.548	0.826	0.491	0.730	0.604	0.708	0.602	0.632	0.648	0.805	0.609	0.609	0.746	0.708	0.709	0.674	0.604	0.759	0.751	0.696	0.630	0.602
Traces (ppm)																								
No. of anal.	1		2	2		1	1	1				2	2	1	3	1	2		1	1	1	2		1
Li	14.5		2.5	7.5		11.5	13.2	16.0				11.7	14.4	15.1	23.6	7.8	4.1		11.7	10.3	5.5	6.6		9.9
Ca	<196		<129	<222		504	<158	<192				281	145	<197	<160	697	289		<218	<308	<334	79		176
Sc	11.7		<1.1	<1.9		4.0	<1.3	<1.6				4.5	<1.3	<1.6	<1.4	9.3	2.1		<1.8	<2.9	<2.9	19.7		3.5
V	60.5		33.1	16.6		28.7	62.7	88.6				36.6	63.2	61.2	11.9	11.8	10.7		64.3	46.6	46.5	80.6		118.0
Cr	4,172		3,51	2,715		2,613	3,607	4,363				3,109	3,827	3,700	1,867	766	842		3,616	1,516	11,316	7,576		5,567
Mn	1,887		2,052	1,916		2,477	2,707	3,079				2,291	2,730	2,693	1,920	1,557	1,598		2,726	1,804	3,650	3,719		3,209
Co	429		293	390		382	555	649				393	546	568	544	400	420		559	488	344	423		360
Ni	6,375		2,758	9,020		7,542	5,606	6,951				8,308	5,392	5,351	7,414	6,328	7,013		5,624	8,309	4,727	8,292		3,766
Cu	n.a.		n.a.	n.a.		n.a.	n.a.	n.a.				n.a.	n.a.	n.a.	n.a.	n.a.	n.a.		n.a.	n.a.	n.a.	n.a.		n.a.
Zn	n.a.		n.a.	n.a.		n.a.	n.a.	n.a.				n.a.	n.a.	n.a.	n.a.	n.a.	n.a.		n.a.	n.a.	n.a.	n.a.		n.a.
Ga	n.a.		n.a.	n.a.		n.a.	n.a.	n.a.				n.a.	n.a.	n.a.	n.a.	n.a.	n.a.		n.a.	n.a.	n.a.	n.a.		n.a.
Ge	n.a.		n.a.	n.a.		n.a.	n.a.	n.a.				n.a.	n.a.	n.a.	n.a.	n.a.	n.a.		n.a.	n.a.	n.a.	n.a.		n.a.
Sr	1.6		0.1	<0.14		0.4	<0.11	<0.13				0.6	<0.10	<0.17	<0.11	0.2	<0.09		<0.14	<0.2	<0.2	<0.08		<0.11
Y	<0.18		<0.11	0.2		<0.13	<0.14	<0.16				0.4	<0.13	<0.18	<0.15	0.3	<0.13		<0.20	<0.2	<0.3	<0.12		<0.14
Zr	25.2		0.3	<0.3		0.3	<0.21	2.6				3.1	<0.16	<0.2	0.3	<0.4	<0.15		<0.2	23.7	5.1	23.3		0.3
Nb	4.8		<0.17	<0.2		<0.15	<0.20	8.3				13.1	<0.17	<0.3	0.2	<0.4	<0.19		0.5	2.3	15.2	4.2		<0.21
Ba	<0.7		<0.6	<0.7		<0.7	<0.8	<0.7				2.6	<0.6	<0.7	<0.5	0.6	1.8		<0.8	<1.4	<1.4	<00.6		<0.6
La	<0.12		<0.06	<0.11		<0.09	<0.09	<0.10				0.4	<0.11	<0.11	<0.10	0.2	<0.09		<0.10	<0.15	<0.2	<0.10		<0.10
Ce	<0.07		<0.05	<0.07		<0.07	<0.07	<0.10				0.2	<0.07	<0.08	<0.06	<0.13	<0.05		<0.10	<0.3	<0.13	0.1		0.1
Pr	<0.09		<0.09	0.1		<0.08	<0.09	<0.10				<0.13	<0.09	<0.12	<0.10	<0.21	<0.09		<0.14	<0.17	<0.20	<0.08		<0.11
Nd	<0.4		<0.3	<0.5		<0.3	<0.4	<0.4				0.7	<0.3	<0.6	<0.4	0.3	<0.2		<0.6	<0.8	264.0	<00.3		<0.3
Sm	<0.5		<0.4	<0.6		0.4	<0.5	<0.8				<0.62	<0.4	<0.5	<0.4	<0.9	<0.4		<0.9	<1.0	<0.9	<0.4		<0.5
Eu	<0.20		<0.10	<0.21		<0.17	<0.16	<0.16				<0.22	<0.17	<0.3	<0.14	<0.24	<0.11		<0.17	<0.2	<0.3	<0.14		<0.14
Gd	<0.7		<0.4	<0.5		<0.5	<0.5	<0.5				0.8	<0.7	<0.6	<0.4	<0.9	<0.4		<0.6	<1.0	<0.7	<0.4		<0.5
Dy	<0.4		<0.22	0.2		<0.3	0.2	<0.5				<0.50	<0.3	<0.5	<0.3	<0.9	<0.3		<0.4	<0.5	<0.8	<0.3		<0.4
Ho	<0.12		<0.09	<0.14		<0.11	<0.13	<0.16				<0.15	<0.08	<0.13	<0.09	<0.17	<0.11		<0.16	<0.2	<0.3	<0.10		<0.11
Er	<0.8		<0.4	<0.6		<0.5	<0.6	<0.7				<0.78	<0.6	<0.8	<0.6	1.0	<0.5		<1.0	<1.0	<1.1	<0.6		<0.5
Tm	<0.15		<0.08	<0.12		<0.08	<0.11	<0.13				<0.16	<0.09	<0.14	<0.08	<0.17	<0.08		<0.15	<0.18	<0.2	<0.09		<0.12

Yb	< 0.4		< 0.3	< 0.4		< 0.4	< 0.5	< 0.3				< 0.38	< 0.4	< 0.4	< 0.4	0.3	< 0.4		< 0.7	0.7	< 0.7	< 0.3		< 0.3
Lu	< 0.10		< 0.07	< 0.10		< 0.09	< 0.08	< 0.12				< 0.13	< 0.07	< 0.09	< 0.09	< 0.3	< 0.08		< 0.17	< 0.17	< 0.2	< 00.07		< 0.08
Hf	0.8		< 0.3	< 0.4		< 0.3	< 0.3	< 0.4				< 0.45	< 0.3	< 0.4	< 0.4	< 0.6	< 0.2		< 0.6	< 0.7	< 0.8	1.8		< 0.4
Ta	0.2		< 0.08	< 0.11		0.1	< 0.10	1.1				0.5	< 0.10	< 0.12	0.1	0.1	< 0.08		< 0.17	< 0.18	1.6	1.2		< 0.09
Pb	< 0.5		1.2	< 0.7		< 0.4	< 0.6	< 0.6				5.7	< 0.5	< 0.7	< 0.4	< 1.6	< 0.4		< 0.8	< 1.1	2.2	< 0.4		< 0.4
Th	< 0.18		< 0.10	< 0.16		< 0.12	< 0.14	0.2				3.6	< 0.11	< 0.17	< 0.13	< 0.4	< 0.14		< 0.21	0.3	0.9	< 0.10		< 0.09
U	< 0.09		< 0.07	< 0.07		< 0.10	< 0.12	< 0.13				< 0.12	< 0.06	< 0.11	< 0.08	< 0.18	0.7		< 0.10	< 0.13	< 0.17	0.2		< 0.08

Mineral	fPer	fPer	fPer	fPer	Ilm	Ilm	Ilm	Ilm	Ilm	Ilm	Ilm	Ilm	Ilm	Ilm	Ilm	Pilm	Pilm	Pilm	Spinel	Spinel	Spinel	Spinel	Spinel	Ni**
Sample no.	5–79	5–102	5–103a	5–103b	1–1	1–2	1–4	1–5	1–7	1–8	1–30	1–32	1–34	4–7	5–108	1–3	5–52	5–56	1–35	4–4	5–17a	5–17b	5–55	5–104
Association		SiO_2					fPer		fPer						Maj + Pvk + SiMg						fPer	fPer		CaSi-Pvk
Analyzed	MU	MU	MU	MU	MU	MU	MU	MU	MU	MU	MU	MU	MU	MU	MU	MU	MU	MU	MU	MU	MU	MU	MU	MU
No. of anal.	3	2	2	2	2	1	1	1	2	1	3	1	1	1	1	3	3	3	3	1	3	3	2	1
Wt%																								
SiO_2	0.01	0.00	0.02	0.04	0.00	0.03	0.01	0.06	0.02	0.03	0.07	0.01	0.00	0.00	0.02	0.05	0.06	0.04	0.55	0.55	0.54	0.57	0.56	0.00
TiO_2	< 0.03	< 0.03	< 0.03	< 0.03	50.64	53.40	50.22	54.16	55.06	56.15	55.49	52.51	50.41	51.17	50.13	52.22	51.78	51.93	10.79	10.86	11.12	10.73	10.65	0.07
Al_2O_3	0.08	0.28	0.13	0.24	< 0.02	0.09	< 0.02	0.13	< 0.02	0.07	0.20	0.05	< 0.02	0.04	< 0.02	0.61	0.63	0.47	5.32	5.38	5.25	5.37	5.31	
Cr_2O_3	0.11	1.97	0.77	0.83	< 0.05	< 0.05	< 0.05	< 0.05	< 0.05	< 0.05	0.06	< 0.05	< 0.05	< 0.05	0.06	0.54	0.61	0.66	35.79	36.33	35.45	36.34	36.23	0.01
FeO_{tot}	58.23	31.70	58.90	59.28	47.60	42.79	46.21	40.23	27.55	36.87	40.61	39.62	48.24	45.82	42.43	32.50	32.51	32.72	33.72	33.34	33.44	33.53	33.58	1.29
NiO	0.40	1.00	0.38	0.46	< 0.06	0.12	< 0.06	0.07	< 0.06	< 0.06	0.06	< 0.06	< 0.06	0.10	< 0.06	0.10	0.08	0.11	0.06	0.15	0.06	< 0.06	< 0.06	94.42
MnO	0.34	0.52	0.85	0.94	0.47	0.51	0.73	0.42	11.46	2.12	0.59	5.37	0.44	0.67	6.01	0.24	0.25	0.25	0.77	0.74	0.75	0.79	0.75	0.07
MgO	39.66	62.62	37.04	36.64	0.45	0.57	0.12	0.50	0.19	0.05	0.06	0.81	0.40	0.13	< 0.04	11.79	11.88	11.94	10.54	10.76	10.60	10.72	10.68	0.00
CaO	< 0.03	< 0.03	< 0.03	0.04	< 0.03	0.04	0.03	< 0.03	< 0.03	< 0.03	< 0.03	< 0.03	< 0.03	< 0.03	0.03	< 0.03	< 0.03	< 0.03	< 0.03	< 0.03	< 0.03	< 0.03	< 0.03	0.00
Na_2O	0.02	0.97	0.73	0.78	< 0.04	< 0.04	< 0.04	< 0.04	< 0.04	< 0.04	< 0.04	< 0.04	< 0.04	< 0.04	< 0.04	< 0.04	< 0.04	< 0.04	< 0.04	0.05	< 0.04	< 0.04	< 0.04	0.02
K_2O	< 0.04	< 0.04	< 0.04	< 0.04	< 0.04	0.04	< 0.04	< 0.04	< 0.04	< 0.04	< 0.04	< 0.04	< 0.04	< 0.04	< 0.04	< 0.04	< 0.04	< 0.04	< 0.04	< 0.04	< 0.04	< 0.04	< 0.04	0.21
Total	98.85	99.06	98.85	99.25	99.21	97.55	97.32	95.57	94.28	95.29	97.14	98.38	99.49	97.93	98.67	98.09	97.79	98.15	97.55	98.14	97.21	98.05	97.81	96.08
mg no.	0.548	0.779	0.529	0.524	0.017	0.023	0.005	0.022	0.012	0.002	0.003	0.035	0.015	0.005	0.000	0.393	0.394	0.394	0.358	0.365	0.361	0.363	0.362	
Traces (ppm)						2	1	1	2	2	2	1	1	1	1	1	1	1	2	1	2		1	
No. of anal.																								
Li					< 0.82	2.2	1.8	< 0.86	6.8	4.4	< 0.45	2.6	< 1.04	1.7		1.8	1.2	< 2.5	n.a.	n.a.	n.a.		n.a.	
Ca					< 69.55	< 121.78	< 89.36	< 84.13	< 33.93	< 62.05	< 40.80	< 82.88	< 88.11	< 60.20		< 89.36	< 100.58	< 183.5	n.a.	n.a.	n.a.		n.a.	
Sc					49.7	78.1	24.3	95.0	64.0	69.0	67.3	41.6	46.9	51.3		24.3	21.2	19.9	2.6	5.6	8.5		5.7	
V					240	686	1,534	602	1,129	596	761	402	236	370		1,534	1,499	1,185	4,419	4,345	4,397		4,336.3	
Cr					136	260	2,944	153	146	255	286	148	125	105		2,944	2,833	3,129						
Mn					2,706	3,251	2,397	2,898	39,645	17,084	3,645	13,586	2,772	3,756		2,397	1,558	1,552	5,315	5,210	5,264		5,197	
Co					79	56	155	53	220	139	105	84	77	24		155	146	130	68	71	76		68	
Ni					31	181	790	13	4	59	36	60	37	12		790	739	703	428	423	540		424	
Cu					n.a.	n.a.	n.a.	n.a.	n.a.	n.a.	n.a.	n.a.	n.a.	n.a.		n.a.	n.a.	n.a.	66.8	83.9	176.1		69.2	
Zn					n.a.	n.a.	n.a.	n.a.	n.a.	n.a.	n.a.	n.a.	n.a.	n.a.		n.a.	n.a.	n.a.	106.3	84.7	175.5		169.0	
Ga					n.a.	n.a.	n.a.	n.a.	n.a.	n.a.	n.a.	n.a.	n.a.	n.a.		n.a.	n.a.	n.a.	181.0	173.9	176.8		181.6	
Ge					n.a.	n.a.	n.a.	n.a.	n.a.	n.a.	n.a.	n.a.	n.a.	n.a.		n.a.	n.a.	n.a.	11.2	10.1	16.8		9.9	
Sr					0.2	0.4	0.2	0.3	1.2	0.4	0.3	0.5	0.2	0.7		0.2	0.2	0.3	0.1	0.1	0.3		0.1	
Y					0.3	0.8	0.3	0.5	0.9	0.4	0.4	0.3	0.5	1.4		0.3	0.1	< 0.17	n.a.	n.a.	n.a.		n.a.	
Zr					27.4	56.6	348.7	68.7	194.9	63.1	27.9	55.4	13.1	76.7		348.7	332.1	223.7	82.7	77.1	70.0		79.4	
Nb					335	227	646	205	157	114	125	297	327	455		646	643	840	25.3	23.3	28.9		51.6	
Ba					4.0	3.2	2.3	8.8	43.5	8.4	44.0	5.0	3.2	10.8		2.3	0.3	< 0.8	n.a.	n.a.	n.a.		n.a.	
La					0.6	0.7	0.5	0.8	2.4	2.2	0.7	1.7	0.5	4.9		0.5	< 0.066	< 0.08	n.a.	n.a.	n.a.		n.a.	
Ce					2.1	2.4	1.9	2.9	10.5	3.5	4.1	3.4	2.0	9.7		1.9	0.1	0.2	n.a.	n.a.	n.a.		n.a.	
Pr					0.2	0.2	0.2	0.2	0.8	0.3	0.4	5.2	0.3	0.8		0.2	< 0.068	< 0.11	n.a.	n.a.	n.a.		n.a.	

Table 2 (Contd.)

Mineral	fPer	fPer	fPer	Ilm	Ilm	Ilm	Ilm	Ilm	Ilm	Ilm	Ilm	Ilm	Ilm	Pilm	Pilm	Pilm	Spinel	Spinel	Spinel	Spinel	Spinel	Ni**
Sample no.	5–79	5–102	5–103a	5–103b	1–1	1–2	1–4	1–5	1–7	1–8	1–30	1–32	1–34	4–7	5–108	1–3	5–52	5–56	1–35	4–4	5–17a	5–17b	5–55	5–104
Association		SiO_2					fPer		fPer						Maj + Pvk + SiMg						fPer	fPer		CaSi-Pvk
Analyzed	MU	MU	MU	MU	MU	MU	MU	MU	MU	MU	MU	MU	MU	MU	MU	MU	MU	MU	MU	MU	MU	MU	MU	MU
No. of anal.	3	2	2	2	2	1	1	1	2	1	3	1	1	1	1	3	3	3	3	1	3	3	2	1
Wt%																								
Nd					0.6	2.5	0.7	0.7	3.1	1.0	1.7	0.7	0.7	2.7		0.7	< 0.24	< 0.5	n.a.	n.a.	n.a.		n.a.	
Sm					< 0.24	< 0.39	0.3	0.1	0.5	0.2	0.2	< 0.27	< 0.33	0.3		0.3	< 0.44	< 0.6	n.a.	n.a.	n.a.		n.a.	
Eu					< 0.095	< 0.139	< 0.086	0.0	0.1	0.0	0.1	< 0.071	< 0.103	0.1		< 0.086	< 0.101	< 0.16	n.a.	n.a.	n.a.		n.a.	
Gd					< 0.167	< 0.50	< 0.27	0.1	0.4	0.1	0.2	< 0.20	< 0.31	< 0.24		< 0.27	< 0.23	< 0.4	n.a.	n.a.	n.a.		n.a.	
Dy					< 0.184	< 0.161	< 0.233	0.1	0.3	0.0	0.2	< 0.240	< 0.230	0.4		< 0.233	< 0.224	< 0.4	n.a.	n.a.	n.a.		n.a.	
Ho					< 0.053	< 0.113	0.1	< 0.058	0.1	0.0	< 0.027	< 0.073	< 0.061	0.1		0.1	< 0.091	< 0.09	n.a.	n.a.	n.a.		n.a.	
Er					< 0.28	< 0.49	< 0.31	< 0.32	< 0.163	< 0.22	< 0.165	< 0.34	< 0.37	0.3		< 0.31	< 0.39	< 0.7	n.a.	n.a.	n.a.		n.a.	
Tm					< 0.058	< 0.083	< 0.046	0.0	0.0	0.0	< 0.023	< 0.050	< 0.067	< 0.044		< 0.046	< 0.073	< 0.11	n.a.	n.a.	n.a.		n.a.	
Yb					0.1	< 0.41	< 0.193	0.5	0.3	0.3	0.1	< 0.168	< 0.25	0.6		< 0.193	< 0.30	< 0.4	n.a.	n.a.	n.a.		n.a.	
Lu					0.1	0.1	< 0.059	0.1	0.0	0.1	0.0	0.1	0.1	0.2		< 0.059	< 0.067	< 0.07	n.a.	n.a.	n.a.		n.a.	
Hf					0.8	1.1	13.7	1.3	3.9	1.4	0.7	1.4	0.5	2.0		13.7	14.0	7.7	n.a.	n.a.	n.a.		n.a.	
Ta					22.4	16.0	97.1	14.8	8.6	6.8	8.6	20.3	21.0	34.1		97.1	98.2	124.1	n.a.	n.a.	n.a.		n.a.	
Pb					81.9	96.7	26.0	135.1	316.1	147.0	301.3	89.2	85.9	222.8		26.0	< 0.37	< 0.5	0.9	0.9	11.7		15.2	
Th					20.9	74.6	34.8	74.1	59.1	96.1	33.5	60.8	5.4	62.9		34.8	< 0.075	0.3	n.a.	n.a.	n.a.		n.a.	
U					0.5	0.9	0.4	1.3	2.1	0.8	0.8	0.7	0.4	1.4		0.4	< 0.067	< 0.09	n.a.	n.a.	n.a.		n.a.	

into high- and low-Mn compositions, possibly related to decompression (see below).

Picroilmenites are less abundant in the Juina diamonds (three inclusions, grains no. 1–3, 5–52, and 5–56). These high-Mg ilmenites are similar to many picroilmenite inclusions reported in diamonds from other regions, but are quite low in chromium (0.54–0.66% Cr_2O_3).

The trace-element signatures of the picroilmenites are similar to those of kimberlitic picroilmenites (Griffin et al. 1997), with high contents of Nb, Ta, Zr, Hf, Cr and Ni, but very low levels of REE and LILE. In contrast, the Mn-bearing ilmenites have generally chondritic levels of REE, with a U-shaped chondrite-normalized pattern (Fig. 3), as well as significant levels of Sr, Ba, Th and U. Like the picroilmenites, they have high contents of Nb, Ta, Zr and Hf, but they also have very low Cr and Ni contents compared to kimberlitic ilmenites.

Spinel

Five spinel-group inclusions were extracted from four Juina diamonds (two inclusions were present in no. 5–17 in association with ferropericlase). They are 0.05 to 0.25×0.20 mm in size.

Spinel-group inclusions in diamonds from other regions show a well-defined range of major oxide chemistry with Cr_2O_3 between 56 and 72 wt% (Sobolev 1971). The Al_2O_3 content of chrome spinel inclusions worldwide varies between 3 and 12 wt%, and TiO_2 contents rarely exceed 1 wt% (Sobolev 1971; W.L. Griffin, unpublished data). These features have been considered as diagnostic of chrome spinels associated with diamonds (Sobolev 1971; Vaganov et al. 1999). Table 2 and Fig. 4 show the chemical composition of five spinel inclusions from the Juina area compared with the compositional fields of chrome spinel inclusions in diamonds from other regions (Vaganov et al. 1999). The Juina inclusions have significantly lower Cr_2O_3 contents (< 36.5 wt%), and higher TiO_2 (> 10 wt%) and FeO contents (> 33 wt%). Although their Fe_2O_3 contents (calculated from stoichiometry) are much higher than in other known diamond-related spinels, Fe^{3+}/Fe^{2+} is within the normal range.

The trace-element data emphasize the differences between these spinels and those commonly found in diamonds of lithospheric derivation. Their V and Ga contents are about twice the maximum values found in kimberlitic chromites (Griffin et al. 1994; W.L. Griffin, unpublished data), whereas their Co and Zn contents are less than half the minimum values found in "normal" kimberlitic ilmenites. Their high Nb and moderate Zr contents, however, are similar to those of kimberlitic ilmenites (Griffin et al. 1994).

CaSi-perovskite (CaSiPvk)

Six inclusions of CaSiPvk have been found. Three occur in one diamond (no. 5–104), coexisting with native Ni.

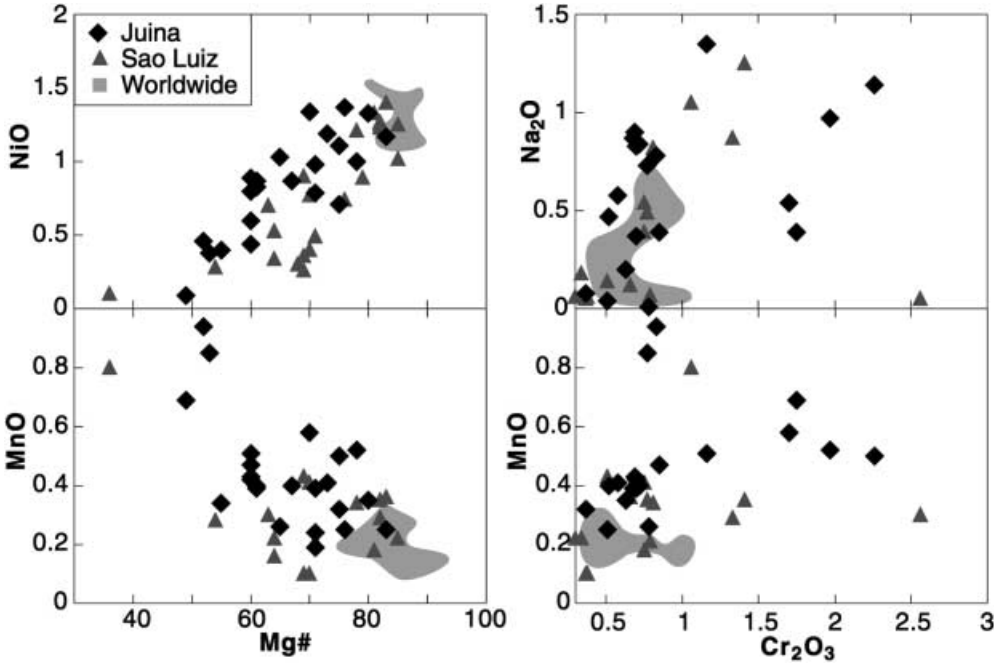

Fig. 2 NiO, MnO, and Na_2O abundances (relative to Cr_2O_3, wt% and Mg#) in ferropericlase inclusions in diamonds from Juina, Sao Luiz (Harte et al. 1999) and worldwide: from Sloan (Otter and Gurney 1989), Koffiefontein (Moore et al. 1986), River Ranch, Zimbabwe (Kopylova et al. 1997), Birim, Ghana (Stachel and Harris 1997), Mwadui, Tanzania (Stachel et al. 1999), Lac des Gras (Davies et al. 1999; Davies, unpublished data), Lesteng-la-Terai (McDade and Harris 1999), and Kankan, Guinea (Stachel et al. 2000b)

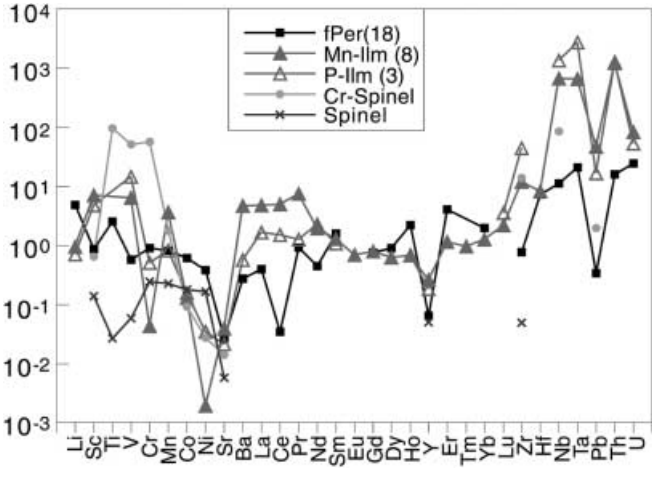

Fig. 3 Averaged chondrite-normalized trace-element abundances of ferropericlase, Mn-ilmenite, picroilmenite (*P-ilm*), Cr-spinel and $(Fe, Mg)_2SiO_4$ inclusions in Juina diamonds. The chondrite-normalized values used here and in Figs. 5 and 7 are those recommended by GERM (www-ep.es.llnl.gov/germ/)

They show little variation in composition, though the largest grain has a slightly lower Ca content. Native Ni was also reported in Sao Luiz diamonds by Wilding et al. (1991), and in DO27 diamonds by Davies et al. (1999).

CaSiPvk is in contact with sphene in no. 5–101, and with "olivine" (see below) in no. 4–101.

The Juina CaSiPvk inclusions are essentially pure $CaSiO_3$, with only traces of other elements, except for grain no. 4–103 which has higher NiO (0.09%), Na_2O (0.12%), and K_2O (0.07%). The CaSiPvk has REE contents ranging from 10–100x chondrites, with an enrichment in the LREE relative to the HREE (Fig. 5). These inclusions differ from the CaSiPvk reported by Harte et al. (1999) in having no positive Eu anomaly, and a greater relative enrichment in LREE. In this regard they are more similar to the CaSiPvk reported from Kankan, Guinea, by Stachel et al. (2000b). The CaSiPvk also contains high but variable levels of Sr, Ba, Zr, Nb, Th and U, but low levels of transition elements.

CaTi-perovskite (CaTiPvk)

CaTi-perovskite (CaTiPvk) is found in association with ilmenite, majoritic garnet (three grains), and an unidentified Si-Mg phase in diamond no. 5–108. To our knowledge, this is the first find of perovskite as an inclusion in diamond. Assuming it to be a syngenetic inclusion, its occurrence together with majoritic garnet indicates derivation from sublithospheric depths (see below). It has an almost stoichiometric composition, with only minor SiO_2 (1.05%), Al_2O_3 (0.64%), and Na_2O (0.33%).

MgSi-perovskite (MgSiPvk)

MgSi-perovskite (MgSiPvk) was found in sample no. 4–104 as a small (100-μm) grain, in contact with a phase interpreted to be TAPP (Harte et al. 1999). The low Ni

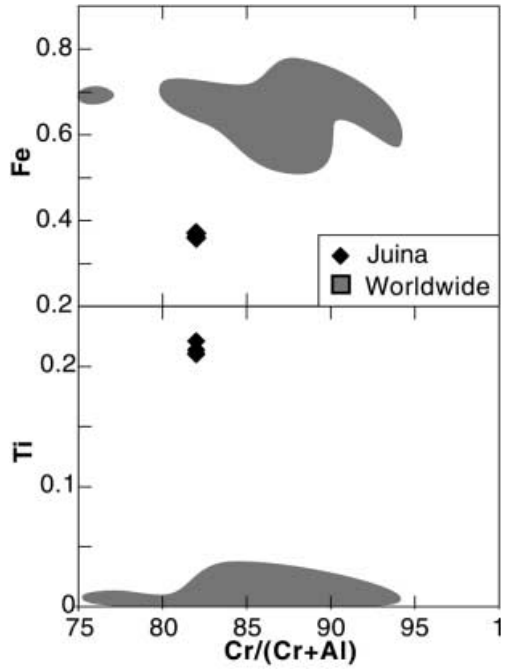

Fig. 4 Fe_{total} and Ti (cations) versus Cr/(Cr + Al) of Cr-spinel in diamonds from Juina and the literature (*shaded area*; $n = 210$)

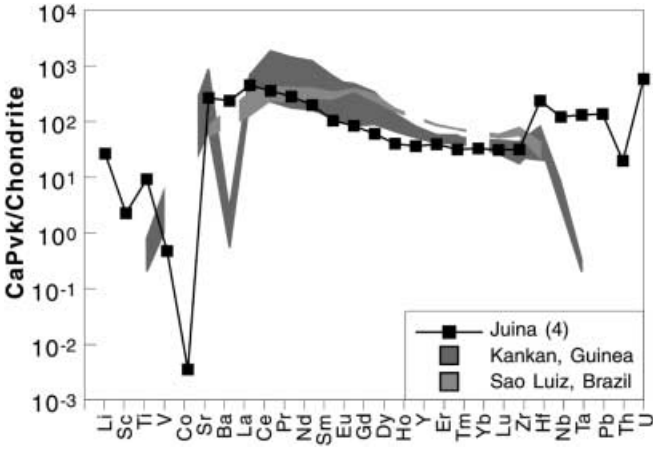

Fig. 5 Averaged chondrite-normalized trace-element abundances of CaSi-perovskite inclusions in Juina diamonds, compared to the range of values in similar inclusions from Sao Luiz (Harte et al. 1999) and Kankan, Guinea (Stachel et al. 2000b)

content of this inclusion (Table 3) is not consistent with it being a peridotitic enstatite. It is similar in FeO and Al_2O_3 contents to the most iron-rich MgSiPvk reported by Harte et al. (1999) and, like that example, it coexists with an inferred TAPP inclusion. The inferred TAPP inclusion analyzed here has higher TiO_2 (7.55 vs. 4.2%) and lower Al_2O_3 (17 vs. 20.2%) than that described by Harte et al. (1999) as coexisting with MgSiPvk and iron-rich fPer, and also has a lower *mg* value (0.812 vs. 0.940). Its identification is based on its association with MgSiPvk and its anisotropy (both of which make it unlikely to be garnet) as well as its composition, especially the low Ca and very low Cr, which are similar to those reported by Harte et al. (1999).

Majorite garnet

Majorite garnet was found as three grains associated with CaTiPvk in a single diamond (no. 5–108). The mean compositions of the three grains show a range in CaO from 10.94–12.18%. However, two of the grains are significantly heterogeneous in composition, with CaO varying in the range 9.75–12.1% in no. 5–108c ($n = 5$), and 9.4–12.0% in no. 5–108b ($n = 2$). In these spot analyses, CaO and MgO are inversely correlated. TiO_2 varies from 1.5–3.2%, and shows no correlation with CaO or MgO. X_{Si} varies from 2.99–3.18 (Fig. 6), and it is positively correlated with CaO content. This pattern of compositional variation is similar to that described by Wilding et al. (1991) who interpreted it as reflecting a very small-scale unmixing of clinopyroxene from the garnet structure. In the present sample no discrete grains of cpx were observed to coexist with the majorite. The trace-element analysis of the majorite shows a flat REE pattern, with significant levels of Sr, Zr and Nb but low contents of transition elements (Fig. 7). The REE pattern is distinctly different from the LREE-depleted patterns shown by majoritic garnets from the Monastery Mine (Moore et al. 1991), but similar flat patterns were reported for Sao Luiz majorite inclusions by Harte (1992), and for Kankan majorite inclusions (Stachel et al. 2000b).

"Olivine"

Three colorless inclusions with the composition of olivine were found in the Juina diamonds. One of them (no. 5–5) occurs in the same diamond as a ferropericlase inclusion, though the two inclusions are not in contact. Another (no. 4–101) occurs in association with CaSiPvk. This association confirms the "olivine" as a member of the lower-mantle assemblage, and implies that the "olivine" may originally have been another high-pressure phase (see below).

Olivines occurring as diamond inclusions worldwide (Fig. 8) fall within well-defined limits in composition, with 91–95 mol% forsterite and minor amounts of Cr_2O_3 (0.05–0.15 wt%), CaO (0.02–0.03 wt%) and NiO (0.25–0.35 wt%). The three Juina inclusions have forsterite contents (87–89 mol%) lower than those of typical diamond-inclusion olivines, and at the low end of the range for olivine in mantle peridotites (O'Reilly et al. 1997). All of the Juina "olivine" inclusions have high Ca contents compared to typical mantle olivines. Two analyzed by LAM-ICPMS contain 1,300–1,900 ppm Ca, whereas the one coexisting with CaSiPvk contains 0.06% CaO (EMP analysis). Compared to typical mantle-derived olivines of similar FeO content, the Ni contents of the Juina olivines

are in the same range, whereas their Zn contents are 25–30% higher and their Mn contents are 50% lower (O'Reilly et al. 1997). Compared to other diamond-inclusion olivines worldwide, the Juina phases also have high Cr contents (Fig. 8). Contents of HFSE and REE are below detection in most cases.

A similarly low-Mg olivine ($Fo_{88.4}$) has been reported as a diamond inclusion in the Canadian DO27 kimberlite pipe where numerous ferropericlase inclusions were found (Davies et al. 1999). A single olivine inclusion with $Fo_{78.8}$ composition was found in the Jagersfontein kimberlite (Chinn et al. 1998). Wilding et al. (1991) reported an olivine inclusion of Fo_{85} composition in a diamond from Sao Luiz. If our interpretation of this phase is correct, these other reports of Fe-rich "olivine" from localities containing superdeep diamonds may also represent an inverted superdeep phase. This suggestion could be tested by trace-element analysis. Figure 8 shows that some of these "olivine" inclusions have low Ni and high Mn compared to olivine inclusions from localities without fPer-bearing diamonds.

SiO_2

A SiO_2 phase was found in three specimens (nos. 4–102, 5–102, and 5–107). It is virtually pure SiO_2. Minor NiO (0.06%) is present in this phase in sample no. 5–102 where SiO_2 is associated with ferropericlase. Because of this paragenesis, and by analogy with other SiO_2 inclusions found in the superdeep association, we assume that this phase may originally have formed as stishovite.

Native Ni

Native Ni was found in association with CaSiPvk in sample no. 5–104. It has approximately 1% Fe admixture and minor amounts of Ti and Mn. The presence of potassium (0.21%) is a remarkable (and unexplained) feature of this Ni grain. Native Ni was also reported in Sao Luiz diamonds by Wilding et al. (1991), and in DO27 diamonds by Davies et al. (1999).

Sphene (titanite)

Sphene (titanite) was recorded as a large (300-μm) grain in association with CaSiPvk in sample no. 5–101. The two phases are in contact, implying a superdeep origin for the titanite. This is in contrast to the recently reported "sphene" inclusion, associated with magnetite, in a Dokolwayo diamond (Daniels and Gurney 1999). The TiO_2 content is low, which suggests the presence of other elements (the phase has not been analyzed by LAM-ICPMS). We do not have crystallographic data on this inclusion. Assuming that it is a syngenetic inclusion, we speculate that it may represent a high-pressure polymorph of $CaTiSiO_5$, bearing the same relationship to titanite as the TAPP does to almandine-pyrope garnet.

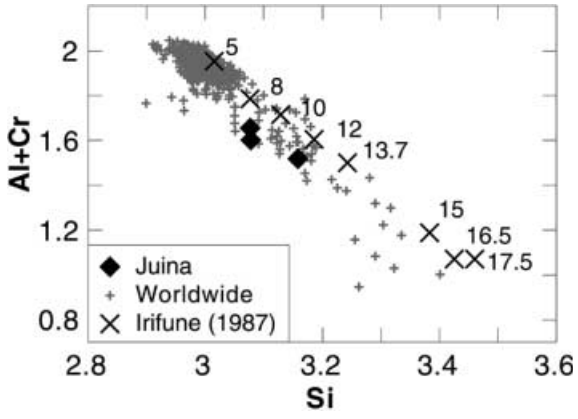

Fig. 6 Al + Cr versus Si (atomic proportions calculated from 12 oxygen) for majorite garnets from Juina, compared with worldwide eclogitic garnet inclusions in diamond ($n = 610$). *Crosses* Experimental data of Irifune (1987), labelled with pressure (GPa)

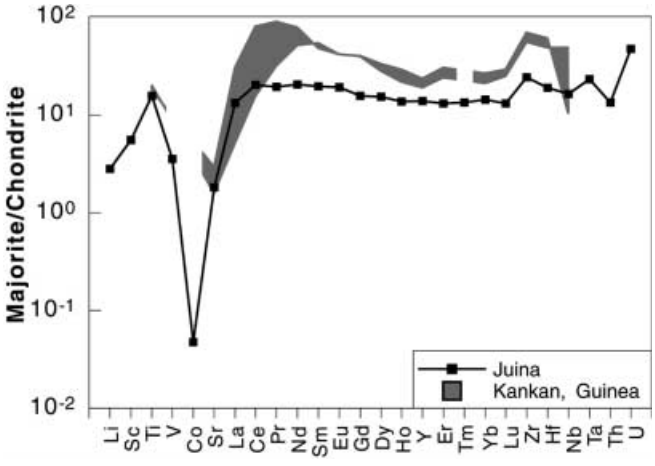

Fig. 7 Averaged chondrite-normalized trace-element abundances in majoritic garnet inclusions from Juina diamonds compared to those from Kankan, Guinea (Stachel et al. 2000a)

Si-Mg phase

An unidentified Si-Mg phase was found in association with ilmenite, majorite and perovskite in sample no. 5–108. No elements other than Mg and Si were recorded in the phase, which gives a low analytical sum suggesting the presence of volatile components.

Carbon-isotope composition of diamonds

Eighty-two representative diamonds from the Juina area, 31 of them with mineral inclusions, have been analyzed for carbon-isotope composition (Table 4 and Fig. 9). For some specimens two or more chips were analyzed. These diamonds appeared to be homogeneous in carbon isotopic composition, the difference between the chips not exceeding 0.4‰.

Table 3 Silicate mineral composition for Juna diamond inclusions (all grains were analyzed at Macquarie University). *n.a.* Not analyzed

Mineral	CaSiPvk	CaSiPvk	CaSiPvk	CaSiPvk	CaSiPvk	CaSiPvk	CaTiPvk	MgSiPvk	TAPP	Majorite	Majorite	Majorite	"Olivine"	"Olivine"	"Olivine"	Titanite	Si-Mg phase
Sample no.	4–101	4–103	5–101	5–104a	5–104b	5–104c	5–108	4–104	4–104	5–108a	5–108b	5–108c	4–101	5–5	5–54	5–101	5–108
Grain size (μm)	300		300	30	100	90	20	100	200	70		120		80	400	300	30
Association	"Olivine"		Titanite	Ni	Ni	Ni	Ilm + Maj + SiMg	TAPP	MgSiPvk	Ilm + Pvk + SiMg	Ilm + Pvk + SiMg	Ilm + Pvk + SiMg	CaSiPvk	fPericl		CaSiPvk	Ilm + Maj + Pvk
No. of anal.	1	1	2	2	1	2	2	4	2	2	2	5	3	4	4	2	2
Wt%																	
SiO_2	51.11	51.90	50.72	51.23	53.51	50.62	1.05	55.96	37.75	42.46	41.46	40.98	41.03	40.31	40.40	33.04	61.95
TiO_2	0.03	0.04	0.03	0.04	0.05	< 0.03	55.64	0.23	7.55	1.83	1.95	2.36	< 0.03	< 0.03	< 0.03	29.70	< 0.03
Al_2O_3	0.11	0.04	0.05	0.06	0.03	0.06	0.64	2.16	16.96	17.22	18.82	18.03	0.03	0.03	0.03	3.16	0.10
Cr_2O_3	< 0.05	< 0.05	< 0.05	< 0.05	< 0.05	< 0.05	< 0.05	0.17	1.74	0.10	0.12	0.07	0.22	0.15	0.24	< 0.05	< 0.05
FeO_{tot}	0.03	0.04	0.06	0.06	0.03	0.01	0.07	8.57	10.06	12.68	13.37	14.20	12.05	10.79	11.84	0.06	0.34
NiO	< 0.06	0.09	< 0.06	< 0.06	< 0.06	< 0.06	< 0.06	< 0.06	< 0.06	< 0.06	< 0.06	< 0.06	0.38	0.45	0.36	< 0.06	< 0.06
MnO	< 0.05	< 0.05	< 0.05	0.05	< 0.05	< 0.05	< 0.05	0.20	0.16	0.23	0.30	0.25	0.10	< 0.05	0.14	< 0.05	< 0.05
MgO	0.00	< 0.04	< 0.04	< 0.04	< 0.04	< 0.04	< 0.04	32.26	24.39	12.30	12.46	11.88	47.27	47.42	47.01	< 0.04	30.33
CaO	48.74	45.91	47.60	48.37	45.80	47.99	40.54	0.03	< 0.03	12.18	10.70	11.12	0.06	< 0.03	< 0.03	27.75	< 0.03
Na_2O	< 0.04	0.12	0.05	< 0.04	< 0.04	< 0.04	0.33	0.10	< 0.04	0.88	0.67	0.61	0.09	0.04	0.04	< 0.04	< 0.04
K_2O	< 0.04	0.07	< 0.04	< 0.04	< 0.04	< 0.04	0.11	< 0.04	< 0.04	< 0.04	< 0.04	< 0.04	< 0.04	< 0.04	< 0.04	< 0.04	< 0.04
Total	100.02	98.20	98.51	99.81	99.42	98.68	98.37	99.68	98.62	99.88	99.85	99.50	101.22	99.19	100.06	93.70	92.71
mg no.								0.870	0.812	0.633	0.624	0.599	0.875	0.887	0.876		0.994
Traces (ppm)																	
No. of anal.			2		2					2				1	1		
Li			2.5		50.5					7.2				n.a.	n.a.		
Ca			n.a.		n.a.					n.a.				1,315	1,866		
Sc			10.4		20.6					47.5				1.2	< 0.65		
Ti			n.a.		n.a.					n.a.				20.6	14.7		
V			34.9		44.8					300				3.89	6.18		
Cr			n.a.		n.a.					n.a.				897	1,047		
Mn			n.a.		n.a.					n.a.				625	718		
Co			0.62		< 2.9					36.4				143	131		
Ni			n.a.		n.a.					21.4				2,922	2,501		
Zn			n.a.		n.a.					n.a.				88.2	80.0		
Ga			n.a.		n.a.					n.a.				0.515	< 0.59		
Sr			6096		156					14.0				0.137	< 0.029		

Y	130	36.8	31.2	0.097	0.130
Zr	154	1,483	133	0.545	<0.104
Nb	52	19.9	6.1	n.a.	n.a.
Ba	5.4	1,423	<0.45	n.a.	n.a.
La	249	69.0	4.9	n.a.	n.a.
Ce	526	144	19.3	n.a.	n.a.
Pr	60.5	15.0	2.6	n.a.	n.a.
Nd	290	50.5	14.5	n.a.	n.a.
Sm	38.2	7.4	4.5	n.a.	n.a.
Eu	12.7	1.6	1.7	n.a.	n.a.
Gd	15.0	6.3	4.8	n.a.	n.a.
Dy	24.3	4.6	5.8	n.a.	n.a.
Ho	4.5	1.4	1.2	n.a.	n.a.
Er	11.5	3.5	3.2	n.a.	n.a.
Tm	1.6	0.52	0.48	n.a.	n.a.
Yb	10.9	3.3	3.5	n.a.	n.a.
Lu	1.5	0.65	0.50	n.a.	n.a.
Hf	4.2	36.7	3.4	n.a.	n.a.
Ta	3.8	1.2	0.60	n.a.	n.a.
Pb	1.3	143	<0.20	n.a.	n.a.
Th	6.1	26.5	0.57	n.a.	n.a.
U	4.6	7.3	0.58	n.a.	n.a.

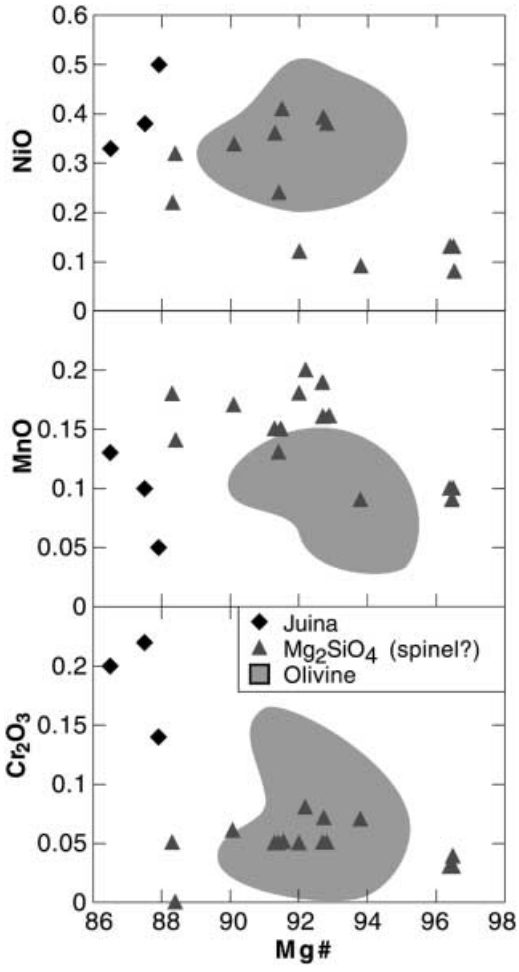

Fig. 8 NiO, MnO and Cr_2O_3 (wt%) versus Mg#, compared with those of olivine inclusions in diamonds from the literature (*shaded area*; $n=377$) and $(Fe, Mg)_2SiO_4$ inclusions in diamonds from Juina and other superdeep diamond localities worldwide (Rickard et al. 1989; Stachel and Harris 1997; Davies et al. 1999; Harte et al. 1999; Stachel et al. 2000b; Davies, unpublished data). Points lying outside the shaded area may have formed as the spinel-structured γ-Mg_2SiO_4 phase in the deep part of the transition zone

No correlation between carbon isotopic composition and diamond morphology was found. This result is consistent with the majority of previous studies (e.g., Deines 1980).

With one exception, the diamonds studied are characterized by a narrow range of carbon isotopic composition varying from $\delta^{13}C=-2.5$ to $-7.8‰$. No differences related to inclusion type are apparent. These values fall within the $\delta^{13}C$ range for diamonds of peridotitic paragenesis ($\delta^{13}C$ from –1 to –9‰), and the mode at –4.9‰ $\delta^{13}C$ (standard deviation $\pm 0.9‰$) is close to the "mantle value" of –4.5 to –5.0‰ (e.g. Galimov 1968; Mattey 1987; Deines 1992). A similar isotopic composition (mode at $\delta^{13}C=-5‰$) was reported for Sao Luiz diamonds of the superdeep paragenesis by Hutchison et al. (1999). The data do not suggest any differences in isotopic composition between the three localities studied. The source material for most of the Juina dia-

Table 4 Carbon isotope composition of the Juina diamonds

Diamond no.	Morphology	Inclusions	$\delta^{13}C$ (‰ PDB)	
			Moscow	CSIRO
Area 1. Rio Sao Luis				
1–1	Dodecahedroid	Ilm	–6.3	
1–2	Dodecahedroid	Ilm	–3.9	
1–4	Dodecahedroid	fPer + Ilm	–4.1	
1–5	Uncertain	Ilm	–5.6	
1–6	Dodecahedroid		–5.0	
1–7	Dodecahedroid	fPer + Ilm	–4.2	
1–8	Combination O-D	Ilm	–5.3	
1–10	Dodecahedroid		–5.1	
1–11	Dodecahedroid		–5.7	
1–12	Dodecahedroid		–5.9	
1–14	Uncertain		–4.1	
1–18	Dodecahedroid		–5.0	
1–21	Dodecahedroid		–5.0	
1–22	Dodecahedroid		–5.3	
1–24	Dodecahedroid		–4.6	
1–27	Combination O-D		–5.0	
1–30	Octahedron	Ilm	–4.9	
1–31	Dodecahedroid	fPer	–5.2	
1–32	Dodecahedroid	Ilm	–5.3	
1–33	Octahedron	fPer	–4.5	
1–34	Uncertain	Ilm	–3.9	
1–35	Dodecahedroid	Spinel	–7.8	
1–36	Octahedron	fPer	–6.9	
1–37	Dodecahedroid		–5.1	
1–38	Dodecahedroid	fPer	–5.0	
Area 4. Rio Vermelho				
4–4	Dodecahedroid	Spinel	–4.5	
4–7	Dodecahedroid	Ilm	–4.5	
4–18	Dodecahedroid	fPer	–3.7	
4–19	Uncertain		–6.8	
4–20	Uncertain		–5.0	
4–21	Uncertain		–5.3	
4–22	Uncertain		–6.1	
4–23	Aggregate of octahedra		–4.4	
4–24	Octahedron		–4.8	
4–25	Dodecahedroid		–4.9	
4–26	Dodecahedroid		–4.9	
4–27	Dodecahedroid		–3.0	
4–28	Dodecahedroid		–4.4	
4–29	Dodecahedroid		–4.3	
4–30	Uncertain		–2.9	
4–31	Uncertain		–5.4	
4–32	Dodecahedroid		–5.1	
4–33	Dodecahedroid	fPer	–4.3	
4–70	Uncertain		–4.3	
4–71	Uncertain		–3.0	
4–72	Uncertain		–2.5	
4–73	Dodecahedroid		–4.3	
4–74	Dodecahedroid		–3.9	
4–101	Uncertain	CaSiPvk + "olivine"		–4.9
4–103	Uncertain	CaSiPvk		–4.8
4–104	Uncertain	MgSiPvk + TAPP		–5.1
Area 5. Corrigo Chicora				
5–3	Combination O-D		–5.0	
5–7	Dodecahedroid	fPer	–5.1	
5–8	Combination O-D		–4.8	
5–11	Aggregate of octahedra		–4.5	
5–13	Octahedron		–4.8	
5–16	Dodecahedroid		–5.6	
5–17	Twin of dodecahedroids	fPer + spinel	–5.1	

Table 4 (Contd.)

Diamond no.	Morphology	Inclusions	$\delta^{13}C$ (‰ PDB)	
			Moscow	CSIRO
Area 5. Corrigo Chicora				
5–20	Uncertain		–6.8	
5–21	Dodecahedroid	fPer	–4.7	
5–26	Combination O-D		–4.2	
5–29	Dodecahedroid		–4.4	
5–30	Uncertain		–4.6	
5–34	Aggregate of octahedra		–6.1	
5–35	Dodecahedroid		–7.8	
5–52	Dodecahedroid	Pilm	–4.3	
5–53	Dodecahedroid		–4.8	
5–54	Dodecahedroid		–5.0	
5–55	Dodecahedroid	Spinel	–4.3	
5–56	Dodecahedroid	Pilm	–4.9	
5–57	Dodecahedroid		–4.8	
5–58	Dodecahedroid		–4.6	
5–59	Dodecahedroid		–5.1	
5–60	Dodecahedroid		–5.2	
5–76	Dodecahedroid		–6.0	
5–77	Dodecahedroid		–5.2	
5–78	Dodecahedroid		–5.6	
5–79	Combination O-D	fPer	–4.9	
5–80	Twin of octahedra		–6.2	
5–101	Uncertain	CaSiPvk + Spene		–4.4
5–104	Uncertain	CaSiPvk + Ni		–4.3
5–108	Uncertain	Maj + Ilm + Pvk + SiMg		–11.4

monds appears to be isotopically homogeneous. No statistically significant differences were observed for diamonds with different mineral inclusions, and stones without inclusions. This supports the idea that the source of carbon for all the lower-mantle diamonds from the Juina area was isotopically homogenous. However, the narrow range of $\delta^{13}C$ by itself cannot serve as an indication of the lower-mantle paragenesis, narrow distributions of $\delta^{13}C$ having been reported for diamonds with "normal" inclusions (e.g. Finsch and Premier; Deines et al. 1989).

Diamond no. 5–108, which contained three majoritic garnet inclusions, has $\delta^{13}C = -11.4$, similar to values for many eclogitic diamonds worldwide. Hutchison et al. (1999) also reported $\delta^{13}C$ values as low as –12.4 in "transition-zone" diamonds from Sao Luiz, containing majoritic garnet inclusions. These data suggest that most of the superdeep diamonds from the Juina area belong to a single population, but that the majorite-bearing "transition-zone" diamonds represent a different population with a different source material, as was suggested by Harte et al. (1999).

A similar range of carbon-isotope composition has been reported for diamonds with superdeep inclusions from other localities. The diamonds with superdeep inclusions from the Canadian DO27 pipe have a $\delta^{13}C$ mode at –4‰, and three type-II diamonds from the same pipe, inferred to be of the superdeep paragenesis, range from –3 to –6‰ $\delta^{13}C$ (Davies et al. 1999). The analysis of

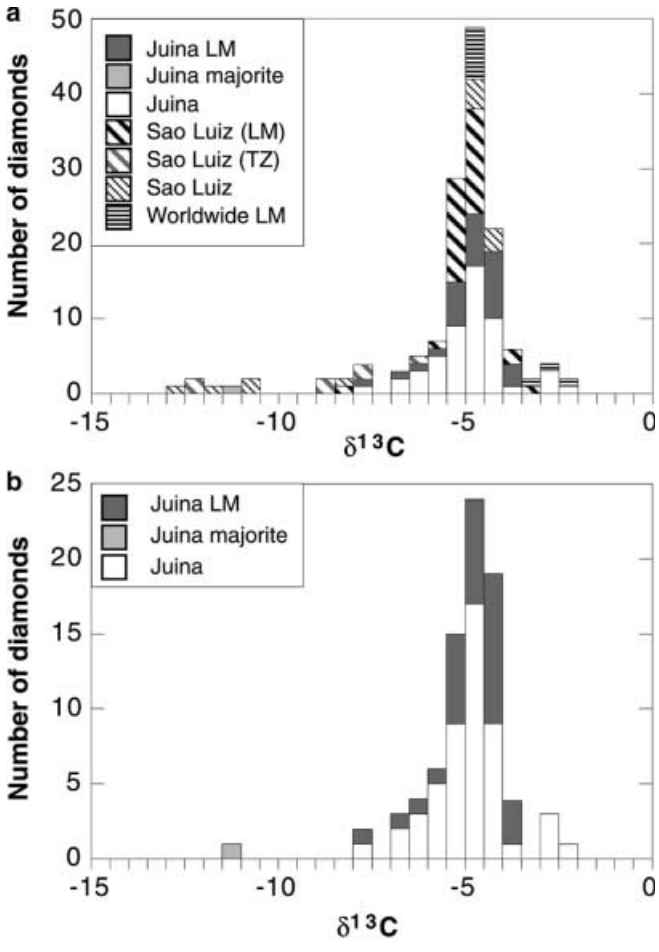

Fig. 9 Carbon-isotope compositions of diamonds from Juina (‰ PDB), compared to diamonds from Sao Luiz (Hutchison et al. 1999) and other localities hosting ferropericlase (Deines et al. 1991; McDade and Harris 1999; Hutchison et al. 1999) and other superdeep phases (Davies et al. 1999). *LM* Lower mantle; *TZ* transition zone

the only diamond from the Letseng-la-Terai pipe with a ferropericlase inclusion gave $\delta^{13}C = -3‰$ (McDade and Harris 1999), and similar isotopic compositions have been found for the Koffiefontein "lower-mantle" diamonds (–5.0 to –5.2‰ $\delta^{13}C$; Deines et al. 1991).

Nitrogen impurities

Structural impurities in 98 Juina diamonds were studied by infrared (IR) spectroscopy. The Juina diamonds contain a large proportion (approximately 45%) of nitrogen-free (type-IIa) diamonds. A- and B-centers in these diamonds do not exceed 20 at. ppm each. Among the remaining 55% of the stones (which may be classed as type-I diamonds), 80% are almost pure IaB with B-center contents usually from 40–205 at. ppm, and up to 460 ppm in one specimen. The A-center, if present (in 20% of type-I diamonds), ranges from 21–42 at. ppm. Only in a few samples does it reach 80–97 at. ppm.

Eighty percent of the diamonds containing nitrogen show platelet degradation with no detectable IR peak. Relatively weak hydrogen-related peaks were detected in many samples. The intensity of the hydrogen-related lines in the IR absorption of diamonds (3,107 and 1,405 cm^{-1}) cannot be used for estimation of the hydrogen content of the diamond. As was demonstrated by Sellschop (1992), and by Sweeney and Winter (1999), the absolute hydrogen content of diamond is not correlated with the IR absorption. It is likely that the above-mentioned lines arise from hydrogen-terminating broken bonds at the internal surfaces (cracks, inclusions, voids, etc.). As was shown by Kiflawi et al. (1996), hydrogen may enter diamond in an optically inactive form, and special annealing converts only part of it to an optically active form.

The FTIR characteristics of the Juina diamonds are comparable to those of the Sao Luiz diamonds, where more than 90% (25 of 36 studied) of "lower-mantle" diamonds are low-nitrogen type-II varieties (average of <20 at. ppm N), whereas eleven diamonds contain aggregated B centers (Hutchison et al. 1999). Type-II diamond is also typical of "superdeep" diamonds from the DO27 kimberlite in Canada, where the only type-I diamond with superdeep inclusions contains nitrogen aggregated to the pure IaB form (Davies et al. 1999). A single diamond with a ferropericlase inclusion from the Letseng-la-Terai pipe, Tanzania is also type-II (McDade and Harris 1999).

At the Institute of Diamonds in Moscow, we have studied many thousands of diamonds from Siberia, Arkhangelsk, South Africa, Venezuela and Brazil. Nitrogen-free and low-nitrogen diamonds comprise approximately 1% of the diamond population in the majority of kimberlite pipes. Only a few exceptions are reported. These include the South African Premier diamonds, which have a high proportion of nitrogen-free diamonds (Smirnov et al. 1986), and diamonds from Jagersfontein (approximately 60% type-IIa; Chinn et al. 1998). In comparison to the worldwide data, the Juina diamonds are distinguished by their low contents of nitrogen and their strongly aggregated B centers. The results of the IR analysis confirm that the superdeep, "lower-mantle" diamonds differ substantially in their nitrogen impurity characteristics from the majority of typical kimberlite-related diamonds studied previously.

Discussion and conclusions

An expanded lower-mantle diamond inclusion paragenesis

The presence of lower-mantle minerals in kimberlites was predicted by Ringwood and Lovering (1970). However, the first real evidence for this hypothesis appeared only when the first ferropericlase inclusions were reported in diamonds from the Orroroo kimberlite,

South Australia, and from the Koffiefontein kimberlite, South Africa (Scott-Smith et al. 1984). These inclusions were interpreted as formed under pressure exceeding 255 kbar, and the authors concluded, "the depth of formation for some diamonds may be considerably greater than previously considered" (Scott-Smith et al. 1984, p. 138). Based on different grounds (density of nitrogen compounds in voidites), Bruley and Brown (1989) also suggested that some diamonds were formed at pressures corresponding to depths of 350–600 km or even deeper.

Harte, Harris and coworkers (Wilding et al. 1991; Harte and Harris 1993, 1994; Harte et al. 1994; Hutchison et al. 1995; Harris et al. 1997; McCammon et al. 1997; Harte et al. 1998, 1999; Hutchison et al. 1999) developed this idea further, based on the study of diamonds from the Sao Luiz placer. These diamonds were believed to be derived from the Cretaceous Aripuena kimberlite province (Wilding et al. 1991). We suppose that these diamonds come from a placer in the southern part of the Juina area (Fig. 1). In addition to ferropericlase, these authors found other superdeep mineral inclusions, analyzed the IR and carbon-isotope characteristics of the Sao Luiz diamonds, and concluded that these diamonds crystallized in the transition zone and the lower mantle.

Single ferropericlase inclusions have been reported from the southern African Monastery, River Ranch and Letseng-la-Terai kimberlite pipes (Moore and Gurney 1989; Kopylova et al. 1997; McDade and Harris 1999). More recently, ferropericlase has been found in diamonds from Tanzanian and North American kimberlite pipes (Otter and Gurney 1989; Stachel et al. 1999; Davies et al. 1999), and in Guinean (Harte et al. 1998; Stachel et al. 2000a, 2000b) and Venezuelan (Kaminsky et al. 1997) placer deposits.

In the absence of the fPer + SiO_2 assemblage, or other coexisting superdeep phases, fPer alone is not necessarily diagnostic of lower-mantle conditions. However, most reported fPer inclusions from localities other than Juina/Sao Luiz have compositions close to those predicted for high-pressure peridotitic assemblages from experimental work (Kesson and Fitz Gerald 1991), and to those known to coexist with SiO_2 or CaPvk (Harte at al. 1999). Such lower-mantle diamond inclusions are known now in almost all diamondiferous provinces (Table 5). In most provinces reports include only a few grains, but at least 15% of all diamond inclusions in the Canadian DO27 pipe are of the superdeep paragenesis (Davies et al. 1999).

The lower-mantle paragenesis reported by Harte and coworkers (summarized by Harte et al. 1999) includes, besides ferropericlase (fPer), two inferred perovskite phases representing high-P polymorphs of $MgSiO_3$ (MgSiPvk) and $CaSiO_3$ (CaSiPvk), a tetragonal polymorph of pyrope garnet (TAPP), and stishovite (SiO_2). The coexistence of fPer + CaSiPvk + MgSiPvk + SiO_2 ± TAPP in this assemblage is consistent with that predicted from experimental studies of peridotitic compositions at high pressure (Kesson and Fitz Gerald 1991; Harte et al. 1999). This assemblage represents the high-pressure equivalent of the olivine, pyroxenes and garnet of typical lithospheric mantle peridotites, at pressures greater than ca. 22 GPa. The assemblage fPer + MgSiPvk + SiO_2 has been reported in diamonds from the

Table 5 Finds of ferropericlase inclusions in diamonds

No.	Province	Locality (pipe, country)	Reference	Number of grains	Association
1	Australia	Orroroo, Australia	Scott-Smith et al. (1984)	2	
2	Southern Africa	Koffiefontein, RSA	Scott-Smith et al. (1984)	4	Enst. MgSiPvk
3		Monastery, RSA	Moore and Gurney (1989)	1	
4		Letseng-la-Terai, Lesotho	McDade and Harris (1999)	1	
5		River Ranch, Zimbabwe	Kopylova et al. (1997)	1	Ecl-Ga
6	Western Africa	Placer deposit, Guinea	Harte et al. (1999)	2	
7		Kankan placer deposit, Guinea	Joswig et al. (1999)	1	CaSiPvk + Opx
8	Eastern Africa	Mwadui, Tanzania	Stachel et al. (1999)	1	
9	Siberia	Udachnaya, Russia (Yakutia)	Zedgenizov et al. (1998)	2	
10		Dianga, Russia (Yakutia)	Sobolev et al. (1999)	2	Ecl-Ga
11		Placer deposit, Russia (Yakutia)	Sobolev et al. (1999)	2	
12	North America	Sloan, USA	Otter and Gurney (1989)	1	
13		DO27, Canada	Davies et al. (1999)	8 (15% incl.)	Ni + $MgSiO_3$
14	South America	Guaniamo placer deposit, Venezuela	Kaminsky et al. (1997)	1	
15		Rio Sao Luiz placer deposit, Brazil	Wilding et al. (1991) Harte and Harris (1994) Harte et al. (1994) Hutchison et al. (1995, 1999) Harte et al. (1998, 1999)	36 (24 anal.)	 Enst, Ca-silicate MgSiPvk, CaSiPvk, TAPP, SiO_2
16		Juina placer deposits, Brazil	This work	28 (>40% incl.) Total = 93 (81 anal.)	Ilm, Sp, Ol, SiO_2

Slave Craton (Davies et al. 1999). The diamonds studied for this report contain all of the inclusion phases previously reported by Harte et al. (1999, and references therein), and the unusual range of *mg* in the present suite of ferropericlases reported by Harte et al. (1999) is replicated in the samples studied here. We therefore consider that the ferropericlases found in this study are of lower-mantle origin, and that phases coexisting with them are of similar origin.

On this basis, we can add five phases, each of which occurs together with ferropericlase and/or CaSiPvk in at least one diamond, to the previously reported inclusion assemblage from this region: low-Mg manganiferous ilmenite, titaniferous chrome spinel, Mg_2SiO_4, native Ni, and titanite. Of the mineral inclusions recognized thus far in the Juina diamonds, only picroilmenite has not been confirmed as belonging to the lower-mantle or transition-zone assemblages.

There are no experimental data on the stability of ilmenite at these pressures, but the ilmenite structure is stable in the $MgSiO_3$ composition at pressures of ca. 22 GPa (Ringwood 1989; Fig. 4). The mineral associations in the Juina diamonds suggest that a range of (Mg, Fe, Mn)TiO_3 phases is also stable in this pressure range, given Ti-rich bulk compositions. Liu (1980a, b) synthesized a polymorph of $MgAl_2O_4$ stable at 20–25 GPa, and Ringwood (1989) suggested that "in the lower mantle, alumina will be contained in this, or a related phase". We suggest that the titaniferous spinel-group phase found in the Juina diamonds (coexisting with fPer) represent such a high-pressure spinel polymorph. This phase has not been observed in experimental studies of peridotite compositions, but it may be stabilized in the relatively Fe, Ti-rich bulk compositions represented by the present inclusion suite. If this is the case, these spinel phases may also provide a residence for Al in parts of the lower mantle.

Olivine is not stable together with fPer in mantle peridotite compositions, but a phase with olivine composition and stoichiometry coexists with fPer in diamond no. 5–5, and with CaSiPvk in diamond no. 4–101. However, a spinel structure is stable in the Mg_2SiO_4 composition just above the 660-km discontinuity (Ringwood 1989; Fig. 4). We therefore suggest that the relatively Fe-, Ca-, Cr-rich "olivine" observed in this study may represent this γ-Mg_2SiO_4 phase. An alternative possibility is that it formed through the decompression reaction fPer + MgSiPvk = olivine. However, this would require that each inclusion originally represented a touching pair of the two high-pressure phases. Given the rarity of touching inclusions in diamonds generally, this appears unlikely.

Harte et al. (1999) noted that the wide range of *mg* in the Sao Luiz ferropericlases contrasts with the narrow range (0.866–0.890) found in most other localities (Fig. 2), and with that predicted by experimental studies of peridotitic compositions (Kesson and Fitz Gerald 1991). They suggested that this might imply a deep-mantle origin for the protolith within which the diamonds crystallized, with extra Fe being added through core-mantle interaction near the "D" boundary. However, the presence of phases such as ilmenite and Ti, Fe-rich Cr-spinel, and even the high Ti content of the TAPP phase, indicate that the rocks in which the Juina diamonds crystallized were also enriched in Ti which is not an obvious signature of core-mantle interaction. In this respect, they are similar to some types of highly metasomatized peridotites known from the lithospheric mantle.

The available trace-element data on the lower-mantle phases from Sao Luiz (Harte et al. 1999; Tables 2 and 3, Figs. 3 and 5) suggest that, relative to the primitive mantle, the parent rock also was significantly enriched in Sr, Ba, LREE, HFSE, and possibly Th and U. In the phases analyzed, Zr/Hf is higher than the chondritic ratio, whereas Nb/Ta is lower. How this enrichment in LIL and HFSE elements has been produced near the 660-km discontinuity is not clear. Mixing with subducted material is a plausible model. A positive Eu anomaly found in the Sao Luiz CaSiPvk (Harte et al. 1999) could support the idea of a subducted origin for the protolith. However, the CaSiPvk inclusions analyzed in this work do not show an Eu anomaly. The overall carbon-isotope homogeneity of the lower-mantle diamonds does not require the addition of crustal material through subduction processes. The ^{13}C-depleted carbon of the one majorite-bearing diamond may provide evidence for the presence of such a recycled crustal component within the transition zone. Further carbon-isotope studies of majorite-bearing diamonds from the area, such as those studied by Wilding et al. (1991), are required to test this suggestion.

Transition-zone inclusions

The occurrence in the Sao Luiz diamonds of majoritic garnets, many partially to completely unmixed to garnet + clinopyroxene, was documented by Wilding et al. (1991), and the two inclusions of this type found here show similar small-scale chemical variation, suggesting partial unmixing of clinopyroxene from majorite. The most Si-rich garnet compositions within diamond no. 5–108 are consistent with derivation from depths of 350–400 km (Fig. 6; Irifune 1987). Given that some cpx has already unmixed from this phase, this is a minimum estimate of the depth of diamond crystallization. The coexistence of this majoritic garnet with CaTi-perovskite and Mn-ilmenite, and the high TiO_2 content of the majorite, indicate a Ti-rich environment of crystallization, and hence a link with the Ti-rich superdeep assemblage discussed above. The occurrence of ilmenite, and especially the Mn-rich ilmenite, in both the "lower-mantle" and "transition-zone" assemblages is a further link between the two. We therefore suggest that diamond no. 5–108 may be derived from the deepest part of the transition zone, near the 660-km discontinuity, and that its majorite inclusions have partially unmixed during ascent. As noted above, the carbon-isotope compo-

sition of this diamond may indicate crystallization from recycled crustal material.

Nitrogen impurities: implications for the source rocks

As noted above, the Juina superdeep diamonds differ from most suites of lithospheric diamonds in having unusually low mean N contents (with nearly half of the samples being type-II diamonds), and in the unusually high degree of B-center aggregation in the diamonds that do contain N at measurable levels. They appear to share these characteristics with other diamonds of the superdeep paragenesis.

It has been well demonstrated that the degree of nitrogen aggregation is a function of temperature and time in both lines Ib–IaA (Taylor et al. 1996) and IaA-IaB (Mendelssohn and Milledge 1995). The high proportion of IaB diamonds among the Juina diamonds indicates that these diamonds had a prolonged high-temperature history, which resulted in the almost complete transformation of single-atomic and paired nitrogen centers into polyatomic complexes of B type. This suggests that diamond crystallization and mantle storage occurred at high temperatures and under high stress.

Another interesting feature of the Juina "lower-mantle" diamonds is that eighty percent of the diamonds containing nitrogen have degraded platelets with no detectable peak. As was shown by Woods (1986), diamonds can be divided into two general types,these being "regular", in which the intensity of platelet peak is proportional to the intensity of absorption by B-defect, and "irregular", where this correlation does not exist. Subsequent studies (Evans et al. 1995) have revealed that "irregular" diamonds contain low amounts of platelets but abundant dislocation loops and voidites. Evans et al. (1995) suggested that, during their post-growth history, "irregular" diamonds underwent annealing under relatively high temperatures, which lead to the degradation of platelets and to the creation of voidites. The present study indicates that many of the Juina diamonds belong to the "irregular" type. This implies that after crystallization a significant fraction of these diamonds was subjected to annealing at high temperatures, probably exceeding that of growth. It would be interesting to check for the existence of voidites in "lower-mantle" diamonds by high-resolution TEM.

The reason for the low nitrogen contents of most superdeep diamonds, from the Juina area as well from other localities, is still a subject of debate. One of the frequently discussed possibilities is that the rocks in the diamond protolith have low nitrogen contents. However, it should be kept in mind that the distribution coefficient of nitrogen between the rock and diamond is a complex function of chemical composition and PT-fO_2 conditions of growth. For example, it has been convincingly demonstrated (e.g. Burns et al. 1999) that the nitrogen content of synthetic diamond strongly depends upon the growth temperature and is inversely proportional to nitrogen solubility in the metal alloy. It is also known that Ti or Zr serve as effective "getters" of nitrogen. The titanium-rich minerals observed in the Juina diamonds might serve as an effective trap for nitrogen, thus decreasing its concentration in the diamond lattice.

Tectonic implications

The presence of lower-mantle diamonds is *prima facie* evidence for plume tectonics, because (in the absence of rapid whole-mantle convection) a mechanism is required to bring these samples from lower-mantle depths to a level (probably < 250 km) where the eruption of kimberlites or other magmas can bring them to the surface (Haggerty 1991, 1999; Griffin et al. 1999). In most places where superdeep diamonds occur, they represent a very small proportion of the diamond population. The great majority of diamonds at these localities appear to be derived from the stable subcontinental lithosphere.

The highest proportion of superdeep diamonds previously reported is from the DO27 kimberlite pipe, Slave Province, where at least 15% of all diamond inclusions are of the superdeep paragenesis, and perhaps 30% of all diamonds may belong to this paragenesis (Davies et al. 1999, unpublished data). The lithospheric section beneath the Slave Province shows an unusually strong compositional layering, with an upper strongly depleted layer separated from a lower layer of more typical Archean composition by a sharp boundary at 150 ± 10 km (Griffin et al. 1999). Griffin et al. (1999) therefore have suggested that the lower part of the strongly layered lithospheric mantle beneath the Slave Province may consist of plume-generated material that rose from the 660-km discontinuity. This model is intended to explain both the compositional layering and the presence of abundant superdeep diamonds. Gaul et al. (2000), by mapping the variation of olivine composition with depth, have shown that similar layering may exist beneath the South Australian and Kaapvaal cratons where superdeep diamonds have been reported, but not beneath the Daldyn kimberlite of Siberia where such diamonds appear to be absent. Further studies are clearly required, but a link between the presence of superdeep diamonds and lithospheric structure, if substantiated, would suggest that plume tectonics have contributed to the development of some lithospheric roots.

The Juina area is unique among known diamond provinces in having a marked predominance of lower-mantle and transition-zone diamonds. The lack of "normal" mineral inclusions (such as pyrope garnet and chromite, or eclogitic phases) in the Juina diamond population, their homogeneous carbon-isotope composition, and the uniformly low nitrogen contents strongly suggest that the overwhelming majority of the diamonds in this area (if not all of them) are of superdeep origin. The Juina sample therefore may be considered as the end-member example of this paragenetic association.

The apparent absence of lithospheric diamonds, or ultramafic and eclogitic paragenesis, suggests that the area did not possess a deep lithospheric root, extending into the diamond stability field, at the time the diamonds were brought to the surface. All diamonds in this area were derived from transition-zone and lower-mantle material raised to the base of the lithosphere, probably through the action of a plume, before eruption of magmatic rocks that brought the diamonds to the surface. The nature of the diamond-inclusion minerals suggests that the diamond-bearing layer thus formed may be of a significantly different composition from the mantle commonly associated with lithospheric diamonds. If this is the case, the nature of "indicator minerals" associated with these diamonds may also not conform to traditional models.

Implications for diamond exploration

Superdeep diamonds may have a much wider distribution than is currently recognized. If these diamonds are brought to the surface by very deep-seated processes, it is not obvious that these processes will occur only beneath areas with thick continental roots, the areas traditionally regarded as prospective for diamond exploration. Some practical consequences of this suggestion may be important.

1. Diamondiferous kimberlites or related diamondiferous rocks may be found not only within areas with thick ancient lithosphere, but also in areas of rather thin lithosphere, underlain by accreted deep material. This may be a key to exploration for primary diamond deposits in areas of placer deposits with "unknown" primary sources.
2. Superdeep diamonds may be associated with indicator minerals other than the "classical" set. Low-Mg olivine, low-Mg high-Mn ilmenite, low-Cr spinel and other minerals should be included in the list of diamond indicator minerals. In such areas, "classical" diamond indicator minerals such as pyrope garnet and high-Cr chromite may be in the minority or absent.
3. The role of high-Cr, low-Ti chromite as the only spinel associated with diamond, and as a criterion of diamond grade in kimberlites, should be reconsidered.

Acknowledgements This work was financially supported by Diagem International Resource Corp., the GEMOC Key Centre, and the Australian Research Council. Prof. S.Y. O'Reilly gave extremely valuable support in organizing the research. F. Kaminsky thanks David Cohen, Paolo Andreazza and other Diagem officials for hospitality and assistance in the Juina area, Brazil. Norman Pearson, Carol Larson and Ashwini Sharma provided valuable assistance with the EMP and LAM-ICPMS analyses at GEMOC, as did Anita Andrew with the C-isotope analyses at CSIRO. We thank Ben Harte and Thomas Stachel for thoughtful and constructive reviews which improved the manuscript. This is publication no. 229 from the ARC National Key Centre for the Geochemical Evolution and Metallogeny of Continents (GEMOC).

References

Boyd SR, Kiflawi I, Woods GS (1994) The relationship between infrared absorption and the A defect concentration in diamond. Philos Mag B69:1149–1153

Boyd SR, Kiflawi I, Woods GS (1995) Infrared absorption by the B nitrogen aggregate in diamond. Philos Mag B72:351–361

Bruley J, Brown LM (1989) Quantitative electron energy-loss spectroscopy microanalysis of platelet and voidite defects in natural diamond. Philos Mag A59:247–261

Burns RS, Hansen JO, Spits RA, Sibanda M, Welbourn CM, Welch DL (1999) Growth of high purity large synthetic diamond crystals. Diamond Related Mater 8:1433–1437

Chinn IL, Milledge HJ, Gurney JJ (1998) Diamonds and inclusions from Jagersfontein kimberlite. Abstr 7th Int Kimberlite Conf, Cape Town, pp 156–157

Daniels LM, Gurney JJ (1999) Diamond inclusions from the Dokolwayo kimberlite, Swaziland. In: Gurney JJ, Gurney JL, Pascoe MD, Richardson SH (eds) Proc 7th Int Kimberlite Conf, vol 1, Cape Town. Red Roof Design, Cape Town, pp 143–147

Davies RM, Griffin WL, O'Reilly SY (1999) Diamonds from the deep: pipe DO27, Slave craton, Canada. In: Gurney JJ, Gurney JL, Pascoe MD, Richardson SH (eds) Proc 7th Int Kimberlite Conf, vol 1, Cape Town. Red Roof Design, Cape Town, pp 148–155

Deines P (1980) The carbon isotopic composition of diamonds: relationship to diamond shape, color, occurrence and vapor composition. Geochim Cosmochim Acta 44:943–961

Deines P (1992) Mantle carbon: concentration, mode of occurrence, and isotopic composition In: Schidlowski M, Golubic S, Kimberley MM, McKirdy DM, Trudinger PA (eds) Early organic evolution: implications for mineral and energy resources. Springer, Berlin Heidelberg New York, pp 133–146

Deines P, Harris JW, Spear PM, Gurney JJ (1989) Nitrogen and ^{13}C content of Finsch and Premier diamonds and their implications. Geochim Cosmochim Acta 53:1367–1378

Deines P, Harris JW, Gurney JJ (1991) The carbon isotopic composition and nitrogen content of lithospheric and asthenospheric diamonds from the Jagersfontein and Koffiefontein kimberlite, South Africa. Geochim Cosmochim Acta 55:2615–2625

Evans T, Kiflawi I, Luyten W (1995) Conversion of platelets into dislocation loops and voidite formation in type IaB diamonds. Proc R Soc Lond A449:295

Galimov EM (1968) Geochemistry of carbon isotopes (in Russian). Nedra Publishing House, Moscow

Galimov EM (1985) The relation between formation conditions and variations in isotope composition of diamonds. Geochem Int (translated from Geokhimiya 8:1091–1118, 1984) 22(1):118–142

Gaspar JC, Teixeira NA, Steele IM (1998) Cathodoluminescence of Juina diamonds. Abstr 7th Int Kimberlite Conf, Cape Town, pp 242–244

Gaul OF, Griffin WL, O'Reilly SY, Pearson NJ (2000) Mapping olivine composition in the lithospheric mantle. Earth Planet Sci Lett 182:223–235

Griffin WL, Ryan CG, Gurney JJ, Sobolev NV, Win TT (1994) Chromite macrocrysts in kimberlites and lamproites: geochemistry and origin. In: Meyer HOA, Leonardos OH (eds) Kimberlites, related rocks and mantle xenoliths. CPRM Spec Publ 1(A/93):366–377

Griffin WL, Moore RO, Ryan CG, Gurney JJ, Win TT (1997) Geochemistry of magnesian ilmenite megacrysts from southern African kimberlites. Proc 6th Int Kimberlite Conf, Novosibirsk. Russian Geol Geophys 38/2:421–443

Griffin WL, Doyle BJ, Ryan CG, Pearson NJ, O'Reilly SY, Davies R, Kivi K, Van Achterbergh E, Natapov LM (1999) Layered mantle lithosphere in the Lac de Gras area, Slave Craton: composition, structure and origin. J Petrol 40:705–727

Haggerty SE (1991) Emplacement implications of ultra-deep xenoliths and diamonds from the transition zone. Abstr 5th Int Kimberlite Conf, Brazil, pp 157–159

Haggerty SE (1999) Diamond formation and kimberlite-clan magmatism in cratonic settings. In: Fei Y, Bertka CM, Mysen BO (eds) Mantle petrology: field observations and high pressure experimentation: a tribute to Francis R (Joe) Boyd. Geochem Soc Spec Publ 6:105–123

Harris JW, Hutchison MT, Hursthouse M, Light M, Harte B (1997) A new tetragonal silicate mineral occurring as inclusions in lower-mantle diamonds. Nature 387:486–488

Harte B (1992) Trace element characteristics of deep-seated eclogitic paragenesis – an ion microprobe study of inclusions in diamonds. Abstr VM Goldschmidt Conf, pp A-48

Harte B, Harris JW (1993) Lower mantle inclusions in diamonds. Abstr Eur Union Geosci, Strasbourg, pp 101 (review Kerr RA (1993) Science 261:1391)

Harte B, Harris JW (1994) Lower mantle mineral associations preserved in diamonds. Min Mag 58A:384–385

Harte B, Hutchison MT, Harris JW (1994) Trace element characteristics of the lower mantle: an ion microprobe study of inclusions in diamonds from São Luiz, Brazil. Min Mag 58A: 386–387

Harte B, Hutchison MT, Lee M, Harris JW (1998) Inclusions of (Mg, Fe)O in mantle diamonds. Abstr 7th Int Kimberlite Conf, Cape Town, pp 308–310

Harte B, Harris JW, Hutchison MT, Watt GR, Wilding MC (1999) Lower mantle mineral associations in diamonds from Sao Luiz, Brazil. In: Fei Y, Bertka CM, Mysen BO (eds) Mantle petrology: field observations and high pressure experimentation: a tribute to Francis R (Joe) Boyd. Geochem Soc Spec Publ 6:125–153

Hutchison MT, Harte B, Harris JW, Fitzsimmons I (1995) Inferences of the exhumation history of lower mantle inclusions in diamonds. Abstr 6th Int Kimberlite Conf, Novosibirsk, pp 242–244

Hutchison MT, Cartigny P, Harris JW (1999) Carbon and nitrogen compositions and physical characteristics of transition zone and lower mantle diamonds from Sao Luiz, Brazil. In: Gurney JJ, Gurney JL, Pascoe MD, Richardson SH (eds) Proc 7th Int Kimberlite Conf, Vol 2, Cape Town. Red Roof Design, Cape Town, pp 372–382

Irifune T (1987) An experimental investigation of the pyroxene-garnet transformation and its bearing on the constitution of the mantle. Earth Planet Sci Lett 45:324–336

Joswig W, Stachel T, Harris JW, Baur WH, Brey GP (1999) New Ca-silicate inclusions in diamonds – tracers from the lower mantle. Earth Planet Sci Lett 173:1–6

Kaminsky FV, Zakharchenko OD, Channer DMD, Blinova GK, Bulanova GP (1997) Diamonds from the Guaniamo area, Bolivar state, Venezuela. Mem VIII Congr Geologico Venezolana. Soc Venezolana Geol, pp 427–430

Kesson SE, Fitz Gerald JD (1991) Partitioning MgO, FeO, NiO, MnO and Cr2O3 between magnesian silicate perovskite and magnesiowustite: implications for the origin of inclusions in diamond and the composition of the lower mantle. Earth Planet Sci Lett 111:229–240

Kiflawi I, Sittas G, Fisher D, Kanda H (1996) The creation of the 3107 cm^{-1} hydrogen absorption peak in synthetic diamond single crystals. Diamond and Related Materials 5:1516–1518

Kopylova MG, Gurney JJ, Daniels LD (1997) Mineral inclusions in diamonds from the River Ranch kimberlite, Zimbabwe. Contrib Mineral Petrol 129:366–384

Liu L (1980a) The pyroxene-garnet transformation and its implication for the 200-km seismic discontinuity. Phys Earth Planet Int 23:286–291

Liu L (1980b) The mineralogy of an eclogitic earth mantle. Phys Earth Planet Int 23:262–267

McCammon C, Hutchison MT, Harris JW (1997) Ferric iron content of mineral inclusions in diamonds from Sao Luiz: a view into the lower mantle. Science 278:434–436

McDade P, Harris JW (1999) Syngenetic inclusion bearing diamonds from Letseng-la-Terai, Lesotho. In: Gurney JJ, Gurney JL, Pascoe MD, Richardson SH (eds) Proc 7th Int Kimberlite Conf, Cape Town. Red Roof Design, Cape Town, pp 557–565

Mattey DP (1987) Carbon isotopes in the mantle. Terra Cognita 7:31–37

Mendelssohn MJ, Milledge HJ (1995) Geologically significant information from routine analysis of the mid-infrared spectra of diamonds. Int Geol Rev 37:95–110

Meyer HOA, Svisero DP (1980) Kimberlites and diamonds in Brazil: windows to the upper mantle. An Acad Brasil Sci 52:819–825

Moore RO, Gurney JJ (1989) Mineral inclusions in diamond from the Monastery kimberlite, South Africa. In: Ross J, Jaques AL, Ferguson J, Green DH, O'Reilly SY, Danchin RV, Janse AJA (eds) Kimberlites and related rocks, vol 2. Proc 4th Int Kimberlite Conf, Perth, 1986. Geol Soc Aust Spec Publ 14. Blackwell, Carlton, pp 1029–1041

Moore RO, Otter ML, Rickard RS, Harris JW, Gurney JJ (1986) The occurrence of moissanite and ferro-periclase as inclusions in diamonds. In: Ext Abstr 4th Int Kimberlite Conf (Geol Soc Aust Abstr 16), Perth, 1986, pp 409–411

Moore RO, Gurney JJ, Griffin WL, Shimuzu N (1991) Ultra-high pressure garnet inclusions in Monastery diamonds: trace element abundance patterns and conditions of origin. Eur J Mineral 3:213–230

Norman MD, Pearson NJ, Sharma A, Griffin WL (1996) Quantitative analysis of trace elements in geological materials by laster ablation ICPMS: instrumental operating conditions and calibration values of NIST glasses. Geostand Newslett 20:247–261

Norman MD, Griffin WL, Pearson NJ, Garcia MO, O'Reilly SY (1998) Quantitative analysis of trace element abundances in glasses and minerals: a comparison of laser ablation ICPMS, solution ICPMS, proton microprobe, and electron microprobe data. J Anal Atomic Spectrosc 13:477–482

O'Reilly SY, Chen D, Griffin WL, Ryan CG (1997) Minor elements in olivine from spinel peridotite xenoliths: implications from thermobarometry. Min Mag 61:257–269

Otter ML, Gurney JJ (1989) Mineral inclusions in diamonds from Sloan diatremes, Colorado-Wyoming State Line kimberlite district, North America. In: Ross J, Jaques AL, Ferguson J, Green DH, O'Reilly SY, Danchin RV, Janse AJA (eds) Kimberlites and related rocks, Vol 2. Proc 4th Int Kimberlite Conf, Perth, 1986. Geol Soc Aust Spec Publ 14, Blackwell, Carlton, pp 1042–1053

Rickard RS, Harris JW, Gurney JJ (1989) Mineral inclusions in diamonds from Koffifontein mine. In: Ross J, Jaques AL, Ferguson J, Green DH, O'Reilly SY, Danchin RV, Janse AJA (eds) Kimberlites and related rocks, Vol 2, Their mantle crust setting. Proc 4th Int Kimberlite Conf, Perth, 1986. Geol Soc Aust Spec Publ 14, Blackwell, Carlton, pp 1054–1062

Ringwood AE (1989) Constitution and evolution of the mantle. In: Ross J, Jaques AL, Ferguson J, Green DH, O'Reilly SY, Danchin RV, Janse AJA (eds) Kimberlites and related rocks, Vol 2. Proc 4th Int Kimberlite Conf, Perth, 1986. Geol Soc Aust Spec Publ 14, pp 457–485

Ringwood AE, Lovering JF (1970) Significance of the pyroxene-ilmenite intergrowths among kimberlite xenoliths. Earth Planet Sci Lett 7:371–375

Scott-Smith BH, Danchin TV, Harris JW, Stracke KJ (1984) Kimberlites near Orroroo, South Australia. In: Kornprobst J (ed) Kimberlites II: the mantle and crust-mantle relationships. Elsevier, Amsterdam, pp 121–142

Sellschop JPF (1992) Nuclear probes in the study of diamonds. In: Field J (ed) The properties of natural and synthetic diamonds. Academic Press, New York, pp 81–180

Smirnov GI, Kaminsky FV, Klyuyev YA (1986) Some features of diamond crystals from the Premier kimberlite pipe, South Africa (in Russian). Mineralogicheskii J 8:69–74

Sobolev NV (1971) On the mineralogy and diamond content of kimberlites. Russian Geol Geophys 3:70–79
Sobolev NV, Yefimova ES, Channer DMD, Anderson PFN, Barron KM (1998) Unusual upper mantle beneath Guaniamo, Guyana shield, Venezuela: evidence from diamond inclusions. Geology 26:971–974
Sobolev NV, Yefimova ES, Koptil VI (1999) Mineral inclusions in diamonds in the northeast of the Yakutin diamondiferous province. In: Gurney JJ, Gurney JL, Pascoe MD, Richardson SH (eds) Proc 7th Int Kimberlite Conf, vol 2, Cape Town. Red Roof Design, Cape Town, pp 816–822
Stachel T, Harris JW (1997) Syngenetic inclusions in diamond from Birim field (Ghana) – a deep peridotitic profile with a history of depletion and re-enrichment. Contrib Mineral Petrol 127:336–352
Stachel T, Harris JW, Brey GP (1999) Rare and unusual mineral inclusions in diamonds from Mwadui, Tanzania. Contrib Mineral Petrol 132:34–47
Stachel T, Brey GP, Harris JW (2000a) Kankan diamonds (Guinea) I: from lithosphere down to the transition zone. Contrib Mineral Petrol 140:1–15
Stachel T, Harris JW, Brey GP, Joswig W (2000b) Kankan diamonds (Guinea) II: lower mantle inclusion parageneses. Contrib Mineral Petrol 140:16–27
Sweeney RJ, Winter F (1999) Kimberlite as high-pressure melts: the determination of segregation depth from major element chemistry. In: Gurney JJ, Gurney JL, Pascoe MD, Richardson SH (eds) Proc 7th Int Kimberlite Conf, Vol 2, Cape Town. Red Roof Design, Cape Town, pp 846–851
Taylor WR, Canil D, Milledge HJ (1996) Kinetics of Ib to IaA nitrogen aggregation in diamonds. Geochim Cosmochim Acta 60:4725–4733
Vaganov VI, Ilupin IP, Kocherov AI (1999) Chrome spinel as indicators of diamond grade (in Russian). Rudi Metall 5:15–31
Wilding MC, Harte B, Harris JW (1991) Evidence for a deep origin for Sao Luiz diamonds. Abstr 5th Int Kimberlite Conf, Brazil, pp 456–458
Woods GS (1986) Platelets and the infrared absorption of type Ia diamonds. Proc R Soc Lond A407:219–238
Zedgenizov DA, Logviniva AM, Shatsky VS, Sobolev NV (1998) Inclusions in microdiamonds from some Yakutian kimberlite pipes (in Russian). Dokl Akad Nauk 359/1:74–79